Prediction of volume of shallow landslides due to rainfall using data-driven models

Tuganishuri Jérémie[1], Chan-Young Yune[2], Gihong Kim[3], Seung Woo Lee[4], Manik Das Adhikari[5], Sang-GukYum[6*]

Department of Civil and Environmental Engineering, Gangneung-Wonju National University,

Corresponding author: Sang-Guk Yum; skyeom0401@gwnu.ac.kr

Abstract

Landslides due to rainfall are among the most destructive natural disasters that cause property damages, huge financial losses, and human deaths in different parts of the World. To plan for mitigation and resilience, the prediction of the volume of rainfall-induced landslides is essential to understand the relationship between the volume of soil materials debris and their associated predictors. Objectives of this research are to construct a model by utilizing advanced data-driven algorithms (i.e., ordinary least square or Linear regression (OLS), random forest (RF), support vector machine (SVM), extreme gradient boosting (EGB), generalized linear model (GLM), decision tree (DT), and deep neural network (DNN), K-nearest neighbor (KNN) and Ridge regression (RR)) for the prediction of the volume of landslides due to rainfall considering geological, geomorphological, and environmental conditions. Models were tested on the Korean landslide dataset to ~~observe~~obtain the ~~best performing model, and among tested algorithms, the~~ most efficient predictions. The extreme gradient boosting ~~ranked high with~~predictions exhibited the highest coefficient of determination (R^2=0.~~85~~8841) and lowest mean absolute error (MAE=~~150.421m^3).~~146.6120 m^3), followed by random forest (R^2=0.8435, MAE=330.4876 m^3). The volume of landslides was strongly influenced by slope length, ~~drainage status~~maximum hourly rainfall, slope angle, aspect, and ~~age of trees~~altitude. The anticipated volume of ~~landslide~~landslides can be important for land use allocation and efficient landslide risk management.

Keywords: Data-driven models, volume of ~~landslide~~landslides, prediction models, rainfall, South Korea

서식 지정함: 글꼴 색: 텍스트 1

서식 지정함: 글꼴 색: 텍스트 1

서식 지정함: 글꼴 색: 텍스트 1

서식 있음: 양쪽, 없음, 오른쪽: 0 cm, 간격 앞: 0 pt, 단락 뒤: 8 pt, 같은 스타일의 단락 사이에 공백 삽입, 단락의 첫 줄이나 마지막 줄 분리 허용, 다음 단락과의 사이에 페이지 나누기, 단어 잘림 허용, 한글과 영어 간격을 자동으로 조절하지 않음, 한글과 숫자 간격을 자동으로 조절하지 않음

서식 지정함: 글꼴 색: 텍스트 1

서식 지정함: 글꼴 색: 텍스트 1

서식 지정함: 글꼴 색: 텍스트 1

서식 지정함: 글꼴 색: 텍스트 1

서식 지정함: 글꼴 색: 텍스트 1

서식 지정함: 글꼴 색: 텍스트 1

서식 지정함: 글꼴 색: 텍스트 1

서식 지정함: 글꼴 색: 텍스트 1

서식 지정함: 글꼴 색: 텍스트 1

서식 지정함: 글꼴 색: 텍스트 1

서식 지정함: 글꼴: 기울임꼴, 글꼴 색: 텍스트 1

서식 지정함: 글꼴 색: 텍스트 1

서식 지정함: 글꼴 색: 텍스트 1

서식 지정함: 글꼴 색: 텍스트 1

1. Introduction

Landslides due to rainfall ~~is~~are phenomena that dislocate a ~~phenomenon in which a given volume~~mass of soil ~~dislocates~~ from its ~~original high to lower point altitude~~ natural position and slide downward along a slope due to gravity forces ~~along a slope fragilized by~~. Intense or long-duration rainfall ~~that~~infiltrates the soil and increases the pore pressure, resulting in soil saturation that leads to slope failure. The saturated soil becomes weak and loses cohesion, and the slope fails when rainfall crosses a certain threshold (Bernardie et al., 2014; Martinović et al., 2018; Lee et al., 2021). ~~This massive volume of soil causes enormous environmental degradation, infrastructure damage, and casualties, which is~~The heavy rainfall saturates a slope and triggers a ~~hindrance~~landslide due to ~~socio-economic aspect~~the reduction of the soil's shear strength and the increase of ~~the community (Van~~pore water pressure (Luino et al.,2022; Chen et al., 2021; ~~Alcántara-Ayala, 2021~~Chatra et al., 2019; Lacerda et al., 2014; Tsai and Chen, 2010). For example, steep slopes with loose soils and even moderate rainfall can lead to the displacement of an enormous quantity of soil mass. On the contrary, in slopes with more stable, cohesive soils, the surface failure might be smaller (Tsai and Chen, 2010). The rainfall quantity and duration influence the volume of the landslides; the higher the intensity and the longer the duration of rainfall, the larger the resulting ~~volume of landslides~~ surface failure (Chen et al., 2017; Bernardie et al., 2014; Chang and Chiang, 2009). The landslide ~~occurrence~~occurrences can also be influenced by human activities that ~~fragilize~~weaken the slope, such as excavation at the slope toe and loading caused by construction and land use such as agriculture, mining etc. (Rosi et al., 2016). ~~Therefore,~~The rapid urbanization activities affect the topography through hill cutting, deforestation and water drainage (Rahman et al., 2017); these activities disturb the slope structure and change the water flow, which exacerbates the effect of landslides in regions where human engineering activities are mostly located (Holcombe et al., 2016; Islam et al., 2017; Chen et al., 2019). ~~accurate prediction of the~~

To estimate the volume of the soil mass displaceable subsequent to intensive rainfall, is essential to set appropriate mitigation strategies to reduce environmental degradation, infrastructure damage, casualties, and to establish post-disaster resilience policies to restore the socio-economic aspect of communities (Van et al., 2021; Alcántara-Ayala, 2021). This quantification of the volume of landslides due to rainfall (VLDR) is essential for effective risk

서식 지정함: 글꼴 색: 텍스트 1

서식 지정함: 글꼴: 굵게 없음, 글꼴 색: 텍스트 1

서식 있음: 양쪽, 없음, 오른쪽: 0 cm, 간격 앞: 0 pt, 단락 뒤: 8 pt, 같은 스타일의 단락 사이에 공백 삽입, 단락의 첫 줄이나 마지막 줄 분리 허용, 다음 단락과의 사이에 페이지 나누기, 단어 잘림 허용, 한글과 영어 간격을 자동으로 조절하지 않음, 한글과 숫자 간격을 자동으로 조절하지 않음

서식 지정함: 글꼴 색: 텍스트 1

서식 지정함: 글꼴 색: 텍스트 1

서식 지정함: 글꼴 색: 텍스트 1

서식 지정함: 글꼴 색: 텍스트 1

서식 지정함: 글꼴 색: 텍스트 1

서식 지정함: 글꼴 색: 텍스트 1

서식 지정함: 글꼴 색: 텍스트 1

서식 지정함: 글꼴 색: 텍스트 1

서식 지정함: 글꼴 색: 텍스트 1

서식 지정함: 글꼴 색: 텍스트 1

서식 지정함: 글꼴 색: 텍스트 1

서식 지정함: 글꼴 색: 텍스트 1

서식 지정함: 글꼴 색: 텍스트 1

서식 지정함: 글꼴 색: 텍스트 1

서식 지정함: 글꼴 색: 텍스트 1

management (Tacconi Stefanelli et al., 2020), emergency response, engineering design (Cheung, 2021), economic assessment and environmental protection (Alcántara-Ayala and Sassa, 2023). Firstly, to manage landslide risk effectively, the quantification of VLDR can be useful for updating hazard maps to reflect the scale of potential landslides in various regions to facilitate the identification of high-risk zones for monitoring and intervention. In addition, to develop mitigation strategies, such as land stabilization measures and land use planning, planners might put in place strict construction regulations in particular regions that are susceptible to landslides (Mateos et al., 2020). The accurate measurements of VLDR can be used to promote public awareness for safety measures and preparedness (Yang and Adler, 2008). Secondly, estimating precise VLDR is crucial for structural engineers to design a structure that can withstand extreme landslide events. Knowing the exact volume of displaceable material, an engineer can set robust stabilization solutions to prevent future occurrences (Dai and Lee, 2001). Moreover, the VLDR can help design the drainage system to manage water flow by controlling groundwater and surface runoff to mitigate landslide risks (Dikshit et al., 2019; Kim et al., 2014). Furthermore, to prepare for emergence responses such as resource allocation, evacuation planning, and search and rescue operations, accurate VLDR estimation is necessary to ensure efficient implementation (Fan et al., 2019). To allocate resources effectively, the volume data is needed to determine the expected number of personnel for evacuation, materials sufficient for cleaning up and recovery (Amatya, 2016; Yang and Adler, 2008; Spiker and Gori, 2003). Further, to establish environmental protection measures such as ecosystem impacts, preservation of soil and water quality, and habitat restoration, the estimates of VLDR are essential (Pradhan et al., 2022; Li et al., 2022a; Barik et al., 2017).

To mitigate the economic impacts of landslides, the values of VLDR can be a basis for estimation of property damages, which is critical for settling insurance claims and assessment of financial impacts on communities and government to facilitate efficient budgeting for repairing damaged infrastructure and restoration of affected parts (Klimeš et al., 2017; Dai et al., 2002). The prediction of the VLDR can assist in long-term economic planning for landslide risk by creating disaster preparedness and recovery funds (Winter and Bromhead, 2012). The accurate estimation of the VLDR is an important key for designing strategies for resilience and planning for the protection of the inhabitants of a particular region with certain landslide risks subjected to a predicted quantity of rainfall (Conte et al., 2022). Consequently, for the safety of communities, the ~~efficient~~ selection of infrastructure construction sites must be done in places ~~where landslides~~

서식 있음: 들여쓰기: 첫 줄: 1.27 cm, 금칙 처리 안 함, 단어 잘림 방지, 문장 부호 끌어 맞추지 않음

서식 지정함: 글꼴 색: 텍스트 1

서식 지정함: 글꼴 색: 텍스트 1

서식 지정함: 글꼴 색: 텍스트 1

~~cannot bury buildings~~with low landslide risks (Fan et al., 2017). Further, for the protection of crops, the farmland location, and other land use activities, accurate landslide prediction taking into account real root causes through the analysis of triggering and influencing factors, is crucial to achieve a durable landslide safety management system (Paudel et al., 2003; Lee, 2009; Fan et al., 2017; Chen et al.,2019; Dai et al., 2019; Alcántara-Ayala, 2021).

~~The prediction of landslide volume due to rainfall is important for the analysis of infrastructure placement to protect against being buried in extreme landslide events. In South Korea, many infrastructures are placed at the foot of mountains, which makes them vulnerable to extreme landslides, which can bury villages, farm lands etc. The findings of Lee (2016) indicated that due to climate change, the average rainfall has increased by 271.23 mm for the period 1971-2100 based on future climate scenarios. Therefore, the efficient prediction of landslide volumes can be useful for land use management in such a way that locations with expected high volume of landslide may be used for other activities which do not get affected by landslide events, such as forest and gardens or activities that reduce water infiltration and non-continuous disturbance of subsoil to maintain groundwater stability and strengthen the topsoil.~~

~~Most researchers focused on the prediction of landslides runout and susceptibility (Giarola et al., 2024; Melo et al., 2019; Peruzzetto et al., 2020). Nevertheless, few researchers estimated the volume of landslides based on the statistical approach (Ju et al., 2023; Dai and Lee, 2001). Ju et al. (2023) constructed an area-volume power law model for the estimation of the volume of landslides using LiDAR data in Hong Kong. Razakova et al. (2020) calculated landslide volume using a digital elevation model and ground-based measurement. Dai and Lee (2001) found that the 12 hours of rainfall influenced the volume of landslides and frequency-volume followed the power law relation. It was observed that most of these studies did not consider detailed predisposing factors and their contribution to the prediction of the volume of landslides due to rainfall. Recently, Lee et al. (2021) applied an artificial neural network (ANN) model for the prediction of the volume of debris flow in the central region of South Korea based on the patterns from the already occurred landslide characteristics and the region morphometry.~~ The prediction of VLDR has gained the interest of many researchers to understand the mechanism and interaction between triggering and aggravating factors. Saito et al. (2014) studied the relationship between rainfall-triggered landslides to test whether the volume of landslides across Japan that occurred between 2001 and 2011 can be directly predicted from rainfall metrics. The findings revealed that larger landslides

서식 지정함: 글꼴 색: 텍스트 1

서식 지정함: 글꼴 색: 텍스트 1

서식 지정함: 글꼴 색: 텍스트 1

occurred when rainfall exceeded certain thresholds, but there were significant discrepancies between peaks of rainfall metrics and maximum landslide volumes, and the total rainfall was the suitable predictor of landslides. Dai and Lee (2001) established the frequency-volume relation for landslides in Hong Kong and noticed that the relation for shallow landslides above $4m^3$ followed the power law. The 12-hour rolling rainfall contributed most to the prediction of the volume of landslides. Ju et al. (2023) constructed an area-volume power law model for the estimation of the volume of landslides using high-resolution LiDAR data collected between 2010 and 2020 in Hong Kong. The aim was to estimate accurately the volume of landslides on small-scale landslides. The reliance on localized datasets limits the model's applicability in regions with different geological settings, and the model does not consider all variabilities of landslide characteristics. Razakova et al. (2020) calculated landslide volume using remote sensed data with the aim of assessing the efficiency of aerial photographs in environmental impact assessment and ground-based measurement. The study did not take into account the effect of vegetation and topography and only focused on a single landslide case, which may be a source of bias due to differences in soil composition and environmental factors. Hovius et al. (1997) analyzed multiple sets of aerial photos and frequency-magnitude relations for landslides in New Zealand. The finding pinpointed that the landslides frequency-magnitude followed power law and infrequent large magnitude contributed to the landscape change. The study also noticed the importance of soil composition in the size of the landslides. This work had a limitation due to the reliance on aerial photos only, which cannot provide accurate measurement in regions of dense forest, and the climatic conditions, which are landslide triggering factors, were not considered, and this may affect the generality of the findings. Guzzetti et al. (2008) applied statistical methods on regional landslide inventories and antecedent rainfall data ranging between 10 min to 35 days. The findings revealed that the slope angle and soil type significantly influence landslide volume estimates, and the rainfall intensity is more important than duration. Chatra et al., 2019) applied numerical methods to study the effect of rainfall duration and intensity on the generation of pore pressure in the soil; the finding revealed a higher instability in loose soil compared to medium soil slopes. The work only treated the interaction of soil and rainfall without considering the environmental factors and human activity, which might also influence mass failure. Recently, the application of GIS technologies has been increasing in the identification of regions susceptible to landslides (landslide zonation) (Chen et al., 2021; Gutierrez-Martin, 2020; Li et al., 2022b). These methods are essential in emergency

management because they provide a general overview of zones with a higher probability of landslide occurrence; however, they do not put emphasis on the determination of the approximate value of the volume of failing mass in relation to excessive rainfall events.

In the present study, the volume of landslides due to rainfall is predicted using OLS, RF, SVM, EGB, GLM, DT, DNN, KNN and RR algorithms, considering the details of triggering factors (i.e., ~~geological,~~ geomorphological, soil and environmental).

~~In this study~~ Here, we aim to construct a data-driven algorithm that combines input parameters for physical-based and empirical models and ~~incorporate~~incorporates more complex non-linear features of input variables to predict the occurrence of associated events more accurately. The main assumption behind the data-driven algorithm is that the considered feature input of the model produces a similar volume of landslides due to rainfall and follows the same pattern at a particular region with the same features under the same quantity of rainfall. Here, we examine different machine learning algorithms and compare their performance using the coefficient of determinations ~~R^2 and mean square errors (MAE) resulting from the application of each algorithm. The model can be customized to be applied in other regions according to the regional settings~~(R^2) and mean square errors (MAE), Root mean square error (RMSE), Mean absolute percentage error (MAPE) and symmetric mean absolute percentage errors of the predicted volume of landslides. The focus is to optimize the predictions of the volume of landslides due to rainfall, taking into account triggering and influencing factors with higher accuracy.

2. Data and Study ~~area~~Region

2.1. Study Region

The region for testing the model is South Korea, characterized by mountainous (63% of total land) relief, especially in the eastern part of the country (Lee et al., ~~2021). The~~ 2022). South Korea is located on the southern part of the Korean ~~peninsula~~Peninsula, bordered by the Yellow Sea to the west coast and the East Sea (Sea of Japan) to the East. According to the Korean Meteorological Administration (2020), the country has a temperate climate ~~comprises cold and dry winters~~characterized by four distinct seasons: hot and humid summers~~.~~, cold winters, and springs and falls with moderate temperatures. The annual rainfall ranges between 1000 mm to 1400mm and 1800mm for the central region and southern region, respectively (Jung et al., 2017; Alcantara

서식 지정함: 글꼴 색: 텍스트 1
서식 지정함: 글꼴 색: 텍스트 1
서식 지정함: 글꼴 색: 텍스트 1
서식 지정함: 글꼴 색: 텍스트 1
서식 있음: 금칙 처리 안 함, 단어 잘림 방지, 문장 부호 끌어 맞추지 않음
서식 지정함: 글꼴 색: 텍스트 1
서식 지정함: 글꼴 색: 텍스트 1
서식 지정함: 글꼴 색: 텍스트 1
서식 있음: 들여쓰기: 첫 줄: 1.27 cm
서식 지정함: 글꼴 색: 텍스트 1
서식 지정함: 글꼴 색: 텍스트 1
서식 있음: 금칙 처리 안 함, 단어 잘림 방지, 문장 부호 끌어 맞추지 않음
서식 지정함: 글꼴 색: 텍스트 1
서식 있음: 금칙 처리 안 함, 단어 잘림 방지, 문장 부호 끌어 맞추지 않음
서식 지정함: 글꼴 색: 텍스트 1
서식 지정함: 글꼴 색: 텍스트 1
서식 지정함: 글꼴 색: 텍스트 1

and Ahn, 2020). During the summer ~~season~~, heavy rainfall from June to September leads to significant surface runoff, increases landslide risk, and causes approximately 95% of all landslides ~~due to rainfall~~ each year (Lee et al., 2020; Park and Lee, 2021). In addition, the landslides may be aggravated by typhoons, which mostly occur in August and September, and it is anticipated that frequency will increase due to climate change~~.~~ (Kim and Park, 2021). The ~~annual~~ rainfall ~~ranges between 1000 mm~~trend analysis from 1971 to ~~1400mm and 1800mm for~~2100 predicted the ~~central region and southern region, respectively (Jung et al., 2017; Alcantara and Ahn, 2020). The geology~~increase in rainfall of 271.23mm, which indicates the ~~Korean peninsula is~~ growing risk of landslides associated with climate change (Lee, 2016). Temperature variations are influenced by its geographical location, the average summer temperatures range between 25 and 30°C, while winter temperatures can drop to -10°C in some parts of the country (Korea Meteorological Administration, 2020). The South Korean geologically is mainly composed of granitic and metamorphic ~~(45%), igneous (30%)~~rocks, such as gneiss, schist, and ~~25% of sedimentary rocks (Lee and Winter,~~granite, which influence the stability of the landscape (Jung et al., 2024). The geomorphology is characterized by rugged mountains, river valleys, and coastal plains, with the Taebaek Mountains running along the eastern edge (Kim et al., 2020). In addition ~~2019). Subsequently~~, the influence of rainfall, environmental, geomorphology, and geological factors ~~frequently generated~~increase the vulnerability to landslides across the country, especially in the northeastern mountainous region, as depicted in Figure ~~1. The distribution of rainfall and volume is summarized in Fig~~ 1.

서식 지정함: 글꼴 색: 텍스트 1

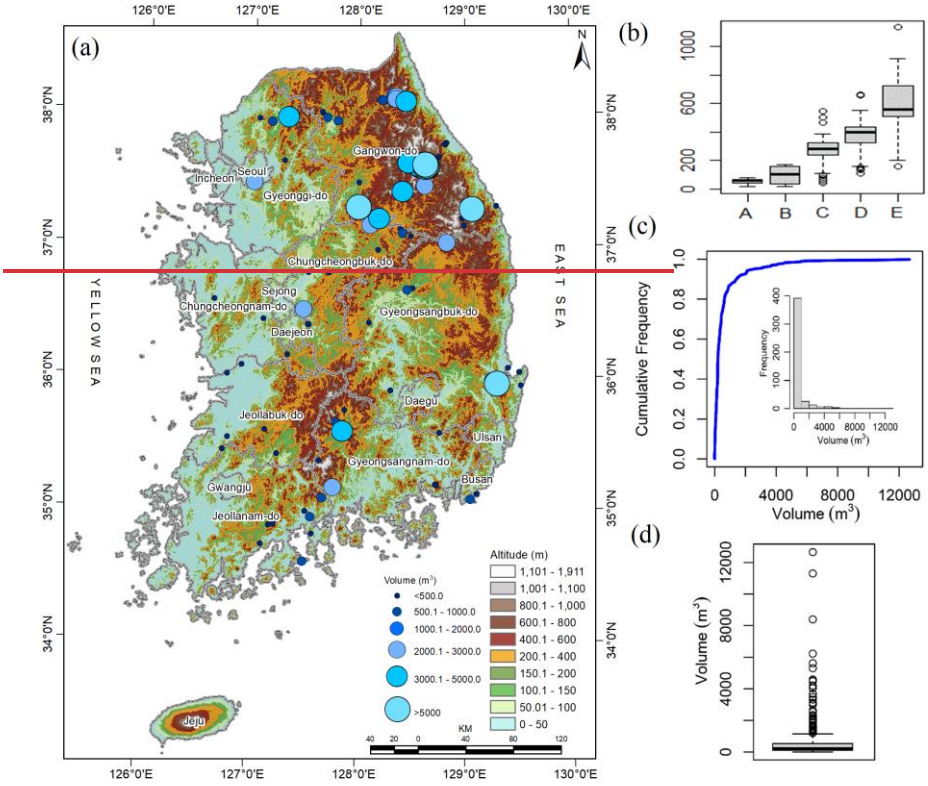

The predominant soil types in South Korea include clay, sandy, and loamy soils, each with different characteristics affecting water infiltration, retention and erosion (Kang et al., 2022; Lee et al., 2023). Clay soils, being more stable, can become highly saturated, increasing landslide risk during heavy rains. On the other hand, sandy soils are more prone to shallow landslides due to fast saturation, leading to instability. Regions with steep topography and poorly consolidated soil (loose) are mostly at risk, especially after prolonged rainfalls (Kim et al., 2015).

Coastal areas are exposed to sea-level rise and coastal erosion, which can further complicate the landscape and increase landslide susceptibility. The combination of heavy summer rainfall, geological composition, and geomorphological factors makes South Korea particularly vulnerable to shallow landslides. Thus, continuous monitoring and research are vital to understand the complex interactions between climate, geology, soil types, and landslide occurrences in this

region (Park, 2022). Understanding the combination of environmental, geological stability, and geomorphological features is crucial for developing effective disaster management strategies and enhancing public safety in landslide-prone areas. As climate change continues to impact rainfall patterns, South Korea faces ongoing challenges in mitigating landslide risks and protecting vulnerable communities.

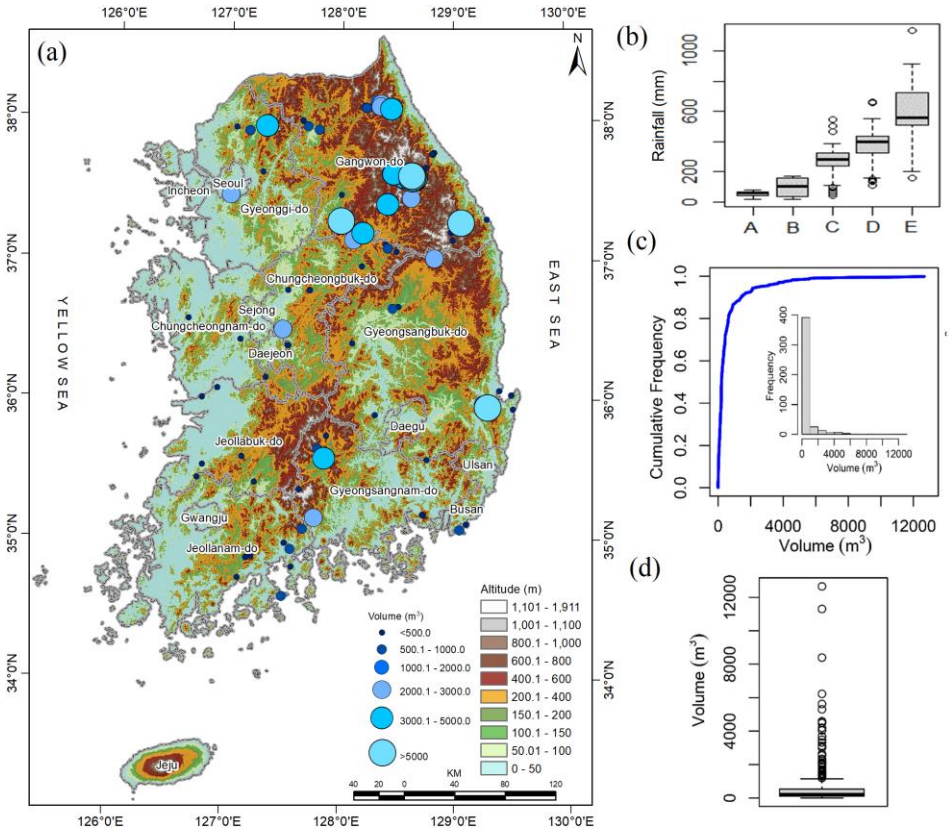

Figure 1. (a) Spatial distribution of landslides in South Korea, (b) temporal variation of rainfall, i.e., A: Maximum hourly rainfall, B: Four weeks rainfall, C: Three hours rainfall, D: Three days rainfall and E: Two weeks rainfall, (c) cumulative frequency distribution of volume of landslides and (d) box plot of volume of landslides.

서식 지정함: 글꼴 색: 텍스트 1

서식 있음: 들여쓰기: 왼쪽: 0 cm, 내어쓰기: 9.9 글자, 금칙 처리 안 함, 단어 잘림 방지, 문장 부호 끝에 맞추지 않음

서식 지정함: 글꼴: 기울임꼴, 글꼴 색: 텍스트 1

서식 있음: 금칙 처리 안 함, 단어 잘림 방지, 문장 부호 끝에 맞추지 않음

~~3.~~*2.2 Data ~~and method~~*

~~In this paper, we consider nine data-driven models, namely ordinary least square or Linear regression (OLS), random forest (RF), support vector machine (SVM), extreme gradient boosting (EGB), generalized linear model (GLM), decision tree (DT), and deep neural network (DNN), k-nearest neighbor (KNN) and Ridge regression (RR) to predict the volume of landslides due to rainfall. The model is tested on the South Korean landslides inventories and predisposing factors coupled with triggering factors, i.e., rainfall data. The detailed workflow is summarized in Figure 2. The steps for construction of these models can be briefly summarized as follows: a) the dataset for landslide inventories is cleaned and joined with rainfall dataset, b) the collinearity analysis is made using variance inflation factor, c) continuous feature are scaled (Z-score) (Bonamutial and Prasetyo, 2023) to facilitate algorithms to converge fast, d) the dataset is split into training and test set, e) all models are tested on the same training set, and the model evaluation on the test set using MAE and R^2 for the comparison of actual and predicted volume by each model, f) variable importance is calculated for most performing model, and g) the distance correlation is calculated for each continuous feature, and Kruskal-Wallis and Dunn test are conducted to examine the similarity of the effect of each category on the landslide volume.~~

서식 지정함: 글꼴: 기울임꼴, 글꼴 색: 텍스트 1

서식 지정함: 글꼴: 기울임꼴, 글꼴 색: 텍스트 1

서식 지정함: 글꼴 색: 텍스트 1

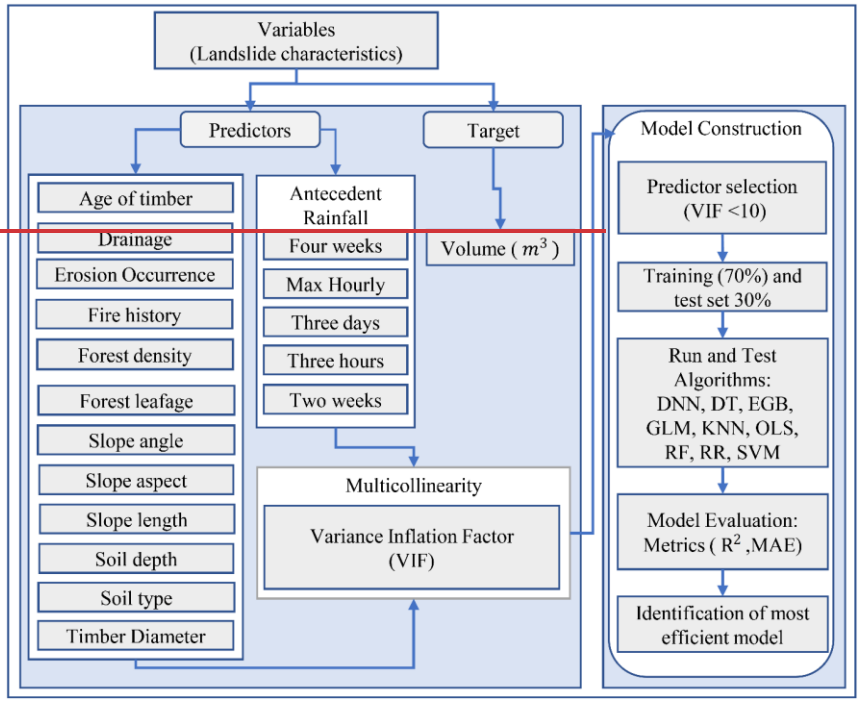

Figure 2.Workflow for the prediction of volume of landslide due to rainfall.

3.1 Data

The landslide inventory dataset contains 450455 landslide record information from 2011 to 2012, which was collected from different locations in South Korea by Korean Forest Services. This dataset tabulates information on landslide location, volume, slopegeometry, such as runout length, soil type, drainage situation, fire history, andwidth, depth, and volume of the affected area, along with geomorphological composition, vegetation features such as age, diameter of timber, leafage, and forest density., and antecedent rainfall prior to landslide events. The details regarding landslide predisposing and triggering factors are summarized in Table 1.

The majority of landslides in this region were shallow, translational slope failures (Kim and Chae, 2009; Kim et al., 2001). The occurred landslides had a volume varying between 1.5m^3 to 12,663m^3 and predominantly occurred in the northeastern and southeastern region (Fig.1a,c & d). The outcome variable (volume) to be predicted was estimated as a product of the area affected

서식 지정함: 글꼴 색: 텍스트 1
서식 지정함: 글꼴 색: 텍스트 1
서식 지정함: 글꼴 색: 텍스트 1
서식 지정함: 글꼴 색: 텍스트 1
서식 지정함: 글꼴 색: 텍스트 1
서식 지정함: 글꼴 색: 텍스트 1
서식 있음: 들여쓰기: 첫 줄: 1.27 cm, 금칙 처리 안 함, 단어 잘림 방지, 문장 부호 끌어 맞추지 않음
서식 지정함: 글꼴 색: 텍스트 1

~~by~~occurred landslides ~~and its depth.~~were hallowed and skewed to the right with 2570.7m^3 as 95th quantile, largest volume was 12,663m^3, and the aggregate mass of landslide due to rainfall was 276,986.62m^3. The estimation of the volume of ~~flown away~~removed material by landslides is important as it ~~help~~helps to assess risks the estimated damage can cause down at the ~~valley at the bottom~~toe of the failed slope, such as blocking transportation network, burying crops or farmland, the damage-built environment near landslide risks area, and post-disaster recovery planning (Evans et al., 2007; Rotaru et al., 2007; Intrieri et al., 2019).

Table 1. Landslide influencing and triggering factors.

Group	Features	Description	Reference
~~Landslides due to rainfall occur as a result of slope failure over saturation from groundwater and rainfall infiltration that destabilize the slope (Kafle, 2022). Therefore~~			
Vegetation	Fire history	The burning of the vegetation intensifies the mass movement of soil near the uncovered burned stem of trees and free movement on uncovered soil due to post-fire rainfall and storms. The sliding may also be due to loss of vegetation, altered soil property and structure, which lead to soil degradation and infiltration which increase pore pressure, and change in hydrology by concentrating water flow in places that exacerbate landslides.	Highland and Bobrowsky, 2008; Culler et al., 2021; Hyde et al., 2016; Stoof et al., 2012
	Age of tree	Mature forests have more resistance to shallow landslides due to highly developed roots, which improve soil cohesion and leaves that prevent direct contact of raindrops with the soil surface.	Sato et al., 2023; Lann et al., 2024
	Forest density	The presence of forest reduces the likelihood of landslides about three times compared to grassland. Grassland has been revealed to be three times more vulnerable to shallow landslides than broadleaf and, coniferous and in secondary forests.	Lann et al., 2024; Greenwood et al., 2004; Turner et al., 2010; Scheidl et al., 2020; Asada et al., 2023
	Timber diameter (m)	Tree spacing and size had been used to investigate the effect of root and tree in shallow landslide control. The high root density generally enhances slope stability,	Cohen and Schwarz., 2017; Wang et al., 2016

서식 지정함: 글꼴 색: 텍스트 1
서식 지정함: 글꼴 색: 텍스트 1
서식 지정함: 글꼴 색: 텍스트 1
서식 지정함: 글꼴 색: 텍스트 1
서식 지정함: 글꼴 색: 텍스트 1
서식 지정함: 글꼴 색: 텍스트 1
서식 지정함: 글꼴 색: 텍스트 1
서식 지정함: 글꼴 색: 텍스트 1
서식 지정함: 글꼴 색: 텍스트 1
서식 지정함: 글꼴 색: 텍스트 1
서식 지정함: 글꼴 색: 텍스트 1
서식 있음: 들여쓰기: 첫 줄: 0 cm, 금칙 처리 안 함, 단어 잘림 방지, 문장 부호 끌어 맞추지 않음
서식 지정함: 글꼴 색: 텍스트 1
서식 있음: 금칙 처리 안 함, 단어 잘림 방지, 문장 부호 끌어 맞추지 않음
서식 있음: 가운데, 줄 간격: 배수 1.15 줄, 금칙 처리 안 함, 문장 부호 끌어 맞추지 않음

		and specific tree placement and root sizes between 5 to 20 mm are effective in landslide prevention.	
Geomorphology	Drainage	The drainage has a significant effect on the slope stability and promotes the efficient control of the influence of rainfall on the ground water fluctuation. The presence of drainage increases the threshold of landslides due to rainfall.	Yan et al., 2019; Sun et al., 2010 ; Wei et al., 2019 ; Korup et al., 2007
	Slope angle (degree)	The steeper slopes have lower presence of landslide due to low transportable materials. Slopes between 20-40 degrees are most vulnerable to greater landslides as rainfall intensity and duration increase. Here, we considered the average angle of the terrain at the landslide location, which provides valuable insight into the region's overall steepness and geomorphic characteristics, which are crucial factors influencing landslide susceptibility and risk modeling.	Duc, 2013 ; Qiu et al., 2016 ; Donnarumma et al., 2013
	Slope aspect	The effect of rainfall on slope differs by slope angle and slope aspect which lead to unevenly distributed occurrence of landslides.	Panday and Dong, 2021; Cellek, 2021
	Slope length (m)	The volume increases as the slope length increases. There exists a complex interplay between rainfall, length of slope and slope angle on the occurrence of landslides.	Turner et al., 2010
	Soil depth (m)	Soil properties, depth, and texture have significant differences in infiltration rates, which have different influences on the occurrence of landslides.	Kitutu et al., 2009; McKenna et al., 2012
	Soil type	Higher rainfall intensity affects the occurrence of landslides differently, particularly in certain soil types that have shorter saturation and failure times.	Liu et al., 2021
Location	Altitude	Regional variability of elevation and mountain steepness affect the quantity of rainfall and associated landslides.	Hyun et al, 2010, Yoon and Bae, 2013; Park, 2015 Um et al., 2010

	Maximum hourly rainfall	The rainfall infiltrates the slope and increases pore water pressure that reduces soil shear strength, which leads to soil saturation that causes surface failure.	Wieczorek, 1987; Smith et al., 2023; Dai and Lee, 2001; Smith et al., 2023
Rainfall	Continuous rainfall	Sudden intense rainfall concentrated in short periods of time is responsible for shallow landslide and debris flow.	Zhang et al., 2019
	Three hours rainfall		
	Three days rainfall	The antecedent rainfalls increase moisture in the soil and weaken soil cohesion.	Ran et al., 2022 Zhang et al., 2019; Bernardie et al., 2014; Chen et al., 2015a; Gariano et al., 2017
	Two weeks rainfall		
	Four weeks rainfall		

Location parameters such as altitude, latitude and longitude are essential elements that determine the microclimate of a given region, influencing rainfall patterns (Hyun et al., 2010; Yoon and Bae, 2013; Park, 2015). The northeastern region is characterized by high-elevation terrain, such as Taebaek, and Sobaek ranges, which dry air and lead to orographic precipitation (Yun et al., 2009). The windward mountain versants receive a substantial amount of rainfall, which can increase the likelihood of landslides (Jin et al., 2022). This variation of rainfall with respect to the direction highlights the importance of including slope aspect variables in landslide studies (Kunz and Kottmeier, 2006). Figure 2(g) depicts the relationship between the slope aspect and the volume of landslides and slope aspect, altitude and fire history and shows that larger volumes were localized in regions that faced forest fire and altitudes between 500 and 1000m. Additionally, the topographical features such as slope length and slope angle affect the size of the landslide (Panday and Dong, 2021), slope failure due to over-saturation from groundwater and rainfall infiltration that destabilize the slope (Kafle et al., 2022). Furthermore, slope length, slope angle and slope aspect play an important role in the determination of the volume of geological material uprooted by landslides (Zaruba and Mencl, 2014; Khan et al., 2021). The slope stability depends on ~~the~~soil composition, properties ~~of composing material which have different~~, including soil permeability ~~index which indicates~~indices that affect water infiltration ~~capability~~and saturation level (Chen et al., ~~2015~~2015a). From surveyed regions, three main soil types, namely, sandy loam, loam, and silt loam, were observed, and their coefficient of permeability is 1.7, 1.65 and 1.5, respectively (Lee

서식 있음: 금칙 처리 안 함, 단어 잘림 방지, 문장 부호 끝에 맞추지 않음

서식 지정함: 글꼴 색: 텍스트 1

서식 지정함: 글꼴 색: 텍스트 1

서식 지정함: 글꼴 색: 텍스트 1

서식 지정함: 글꼴 색: 텍스트 1

서식 지정함: 글꼴 색: 텍스트 1

서식 지정함: 글꼴 색: 텍스트 1

서식 지정함: 글꼴 색: 텍스트 1

et al., 2013~~), were used as numerical predictor variables. In addition,~~). Moreover, to reduce the infiltration drainage network that channeling rainwater ~~in hilly~~ terrain drains soil and reduces the saturation, which minimizes the likelihood of landslide occurrence as a result of groundwater discharge and rainfall water flow (Hovius et al.,~~1998~~ 1997; Wei et al., 2019). Furthermore, the ~~occurrence of forest fires can contribute to the occurrence of landslides due to the burning of~~ vegetation ~~covering the area and can also change soil property and increase soil pH (Lee et al., 2013). Moreover, the vegetation type, leafage, roots, age and density can be predictors of the occurrence and the volume of landslides. The vegetation covers~~protects the topsoil~~, prevents drying and~~ from the direct ~~hit of rain drops which automatically dig holes on~~impact of raindrops hitting the ground, which causes erosion due to the force of gravity ~~acting on the raindrop combined with the soil permeability~~and reduces infiltration (Omwega, 1989; Keefer, 2000). The absence of vegetation allows rainwater to seep away fine topsoil, causing shallow landslides (Gonzalez-Ollauri and Mickovski, 2017). ~~Thus, planting~~On the contrary, vegetation ~~is recommended as a better practice to improve~~improves soil cohesion and ~~prevent~~prevents potential shallow landslides due to soil~~-~~-root interaction (Gong et al., ~~2017~~2021; Phillips et al., 2021). The density of vegetation (forest) and leafage type (broad, pines or mixture) ~~determine~~directly affects the quantity of raindrop intercepted and prevented from directly hitting ~~directly~~ the soil, which emphasizes the vegetation's landslides mitigation role. ~~The rainfall, a triggering factor~~Further, the occurrence of forest fires can contribute to the occurrence of landslides ~~which consists of rainfall at~~due to the ~~time~~burning of ~~landslide event~~vegetation covering the area, changing soil properties and ~~antecedent rainfall are critical factors that influence the occurrence of landslides (Yune~~increasing soil pH (Lee et al., 2013).~~2010; Khan et al.,2012; Kim et al., 2021). In this study, we consider time-based aggregated rainfall. The considered variables are illustrated in Table 1.~~

The rainfall, a triggering factor of landslides, is the immediate cause of slope instability and failure due to infiltration that leads to saturation resulting from increased pore water pressure that reduces soil shear strength (Yune et al., 2010; Khan et al., 2012; Kim et al., 2021; Lee et al., 2021). The antecedent rainfall increases the moisture in the soil, which accelerates the soil saturation; the cumulative effect is essential to understand the saturation levels (Ran et al.,2022). In this study, rainfall variables are grouped based on time, namely, continuous rainfall, which is the accumulative value of rainfall on the day of a landslide from rainfall start hour to the landslide event, maximum hourly rainfall, rainfall during the fixed period such as three hours, one day, three

서식 지정함: 글꼴 색: 텍스트 1
서식 지정함: 글꼴 색: 텍스트 1
서식 지정함: 글꼴 색: 텍스트 1
서식 지정함: 글꼴 색: 텍스트 1
서식 지정함: 글꼴 색: 텍스트 1
서식 지정함: 글꼴 색: 텍스트 1
서식 지정함: 글꼴 색: 텍스트 1
서식 지정함: 글꼴 색: 텍스트 1
서식 지정함: 글꼴 색: 텍스트 1
서식 지정함: 글꼴 색: 텍스트 1
서식 지정함: 글꼴 색: 텍스트 1
서식 지정함: 글꼴 색: 텍스트 1
서식 지정함: 글꼴 색: 텍스트 1
서식 지정함: 글꼴 색: 텍스트 1
서식 지정함: 글꼴 색: 텍스트 1
서식 지정함: 글꼴 색: 텍스트 1
서식 지정함: 글꼴 색: 텍스트 1
서식 지정함: 글꼴 색: 텍스트 1
서식 지정함: 글꼴 색: 텍스트 1
서식 지정함: 글꼴 색: 텍스트 1
서식 지정함: 글꼴 색: 텍스트 1
서식 지정함: 글꼴 색: 텍스트 1
서식 지정함: 글꼴 색: 텍스트 1
서식 지정함: 글꼴 색: 텍스트 1
서식 지정함: 글꼴 색: 텍스트 1
서식 지정함: 글꼴 색: 텍스트 1
서식 지정함: 글꼴 색: 텍스트 1
서식 지정함: 글꼴 색: 텍스트 1
서식 지정함: 글꼴 색: 텍스트 1
서식 지정함: 글꼴 색: 텍스트 1, 프랑스어(프랑스)
서식 지정함: 글꼴 색: 텍스트 1
서식 지정함: 글꼴 색: 텍스트 1, 프랑스어(프랑스)

days, two weeks etc (Fig. 1b). The histograms for rainfall considered in this study are depicted in Figure 2(a-f), and the descriptive statistics for all continuous variables are in Table 2.

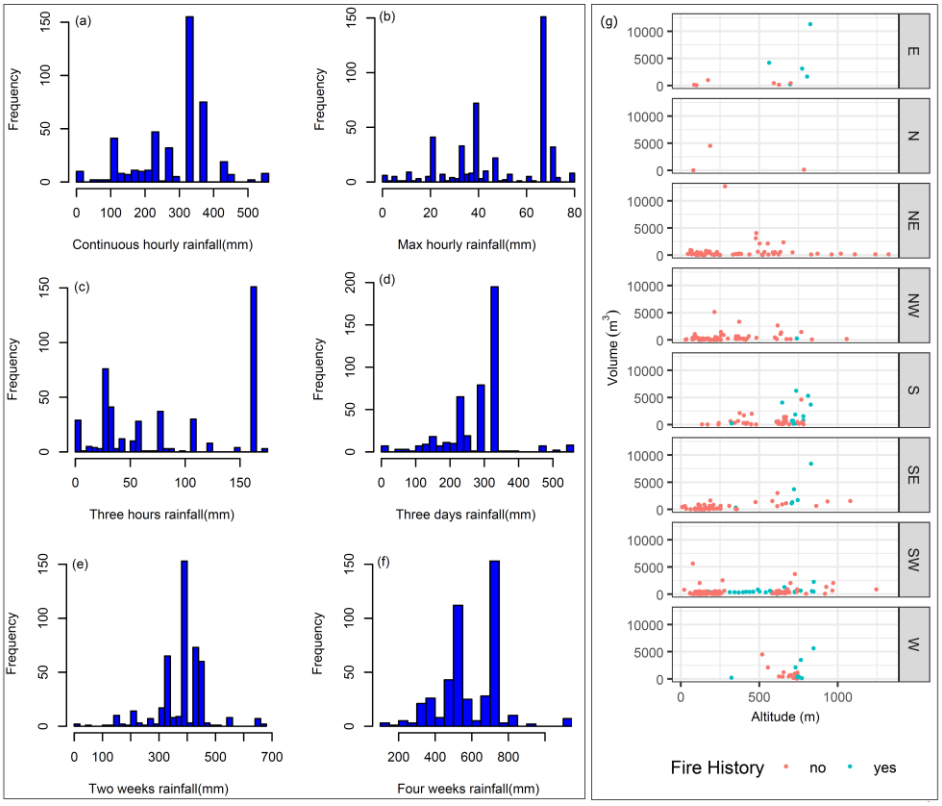

Figure 2. (a-f) Histograms of rainfall data, and (g) the scatter plot showing the variation of landslide volumes with respect to slope aspect, fire history and altitude.

Table 1. Considered variables for data-driven model construction.

Group	Features	Description	Reference
Vegetation	Fire history	The burning of the vegetation intensifies the mass movement of soil near uncovered burned stem of trees and free movement on uncovered soil due to post-fire rainfall and storm.	(Highland and Bobrowsky, 2008; Culler et al.,2021)
	Age of tree Forest leafage Forest density Timber diameter (m)	The age of tree combined with the quantity of rainfall may generate higher landslide intensity especially in in trees of age below 10 years. The disturbance of vegetation significantly impacts the susceptibility of landslides in forested regions.	Turner et al., 2010 ; Scheidl et al.,2020
Geomorphology	Drainage	The drainage has a significant effect on the slope stability and promote the efficient control of the influence of rainfall on the ground water fluctuation. The presence of drainage increases the threshold of landslides due to rainfall.	Yan et al., 2019 ; Sun et al.,2010 ; wei et al.,2019
	Erosion	The presence of erosion increases and contributes to the destructive capability of landslides by increasing the volume of transported materials.	Korup et al., 2007
	Slope angle (degree)	There exists an established relationship between the slope morphology and volume	

서식 지정함: 글꼴 색: 텍스트 1

서식 있음: 들여쓰기: 첫 줄: 0 cm, 금칙 처리 안 함, 단어 잘림 방지, 문장 부호 끌어 맞추지 않음

서식 지정함: 글꼴 색: 텍스트 1

서식 있음: 금칙 처리 안 함, 단어 잘림 방지, 문장 부호 끌어 맞추지 않음

서식 있음: 가운데, 줄 간격: 배수 1.15 줄, 금칙 처리 안 함, 문장 부호 끌어 맞추지 않음

Group	Features	Description	Reference
	Slope aspect Slope length (m)	of landslide due to rainfall. The volume increases as the slope length increases. the steeper slopes have lower presence of landslide due to low transportable materials	Qiu et al.,2016 ; Donnarumma et al., 2013
	Soil depth (m) Soil type	Soil properties, depth and texture have a significant difference in infiltration rates which generate different influence on the occurrence of landslides.	Kitutu et al., 2009 ; McKenna et al., 2012
Rainfall	Maximum rain Four weeks rain Three hours rain Three days rain Two weeks rain	Rainfall intensity has an effect on the volume and frequency of landslides being the major triggering factor. The antecedent rainfall and duration of rainfall influence the volume, and deep landslides happen due to rainfall of long duration.	Wieczorek, 1987; Dai and Lee, 2001; Bernardie et al., 2014; Gariano et al.2017

Variable selection procedure was carried out based on previous literature and applied in the model using variance inflation factor (VIF) (O'Brien, 2007) to eliminate collinear variables. The variable with VIF<10 was considered as non-colinear and hence used in the model. The summary statistics of variables with VIF <10 were summarized in Table 2. The training and test set was scaled (Z-score or variance stability scaling) to solve convergence issues that are associated with running the model without feature scaling (Singh and Singh, 2022). To run the model on the data-data driven methods that accept numerical features, the test and training set was one-hot-encoded to create a feature matrix (Seger, 2018).

Table 2: Summary statistics continuous variables.

서식 있음: 가운데, 줄 간격: 배수 1.15 줄, 금칙 처리 안 함, 문장 부호 끝에 맞추지 않음

서식 지정함: 글꼴 색: 텍스트 1

서식 지정함: 글꼴 색: 텍스트 1

Variable~~Variables~~	units	N	Min	Mean	Median	Max	~~Sd~~Std dev
~~Maximum hourly~~Max Hourly rain	mm	~~450~~455	~~18.50~~	~~52.59648~~	~~61.724~~8	78.~~5~~	~~17.221~~20
Continuous rainfall	mm	455	0	285	327	550	106
Three hours rainfall	mm	~~450~~455	~~150~~	~~95.04488~~	~~105.58~~0	171	~~55.59660~~
Twelve Hours rainfall	mm	455	0	150	99	447	95
One day rainfall	mm	455	0	202	162	538	112
Three days rain	mm	455	0	280	284	550	86
~~Three~~Seven days ~~rainfall~~rain	mm	~~450~~455	~~440~~.5	~~282.31~~32	~~283.53~~	~~549.563~~	~~79.29588~~
~~two~~Two weeks ~~rainfall~~rain	mm	~~450~~455	~~1110~~.5	~~388.3423~~	~~399.54~~	663	~~82.85490~~
Three weeks rain	mm	455	86	504	533	914	115
Four weeks ~~rainfall~~rain	mm	~~450~~455	~~157.91~~08	~~586.0755~~87	561	1135	~~158.6~~160
~~Slope angle~~	~~Degree (°)~~	~~450~~	~~10~~	~~34~~	~~34.004~~	~~65~~	~~7.982~~
~~Slope length~~	~~m~~	~~450~~	~~1.8~~	~~21.246~~	~~13~~	~~180~~	~~22.57~~
Soil depth	m	~~450~~455	~~100~~.2	~~60.3110~~.6	0.75	0.75	~~20.2190~~.19
Soil type	~~constant~~	~~450~~455	1.5	1.~~6756~~	1.~~75~~	1.7	0.~~051~~087
Timber diameter	m	~~450~~455	0.~~11~~15	0.~~22727~~	0.23	0.35	0.~~146~~086
Age of ~~timber~~tree	~~years~~Years	~~450~~455	~~15~~10	~~35.2~~34	35	60	~~13.392~~14

서식 지정함 ... 서식 있음 ... 서식 지정함 ... 서식 지정함 ... 서식 지정함

Variable~~Variables~~	units	N	Min	Mean	Median	Max	~~Sd~~Std dev
~~Volume~~Slope length	~~m~~^{3}m	~~4504~~5	1.~~58~~	~~599.59~~21	~~211.68~~13	~~12663~~1 80	~~1237.128~~23
Slope angle	Degree (°)	455	10	34	34	65	7.9
Altitude	m	455	9	391	272	1324	273

3.~~2 Method~~ Methods

In this paper, we consider nine data-driven models, namely OLS, RF, SVM, EGB, GLM, DT, DNN, KNN and RR to predict the volume of landslides due to rainfall. The model is tested on the South Korean landslides inventories and predisposing factors coupled with triggering factors, i.e., rainfall data. The detailed workflow is summarized in Figure ~~In this study, nine data-driven methods were selected and tested on a Korean dataset. This section contains a brief introduction to each tested method.~~ 3. The steps for construction of these models can be briefly summarized as follows: a) the dataset for landslide inventories is cleaned and combined with rainfall dataset, b) the collinearity analysis is made using variance inflation factor, c) continuous feature are scaled (Z-score) (Bonamutial and Prasetyo, 2023) to facilitate algorithms to converge fast, d) the dataset is split into training and test set, e) all models are tested on the same training set, and the model evaluation on the test set using mean absolute error (MAE), coefficient of determination (R^2), root mean square error (RMSE), symmetric mean absolute percentage error (SMAPE) and mean absolute percentage error (MAPE) for the comparison of actual and predicted volume by each model, f) variable importance is calculated for most performing model, and g) the distance correlation is calculated for each continuous feature, and Kruskal-Wallis and Dunn test are conducted to examine the similarity of the effect of each category on the landslide volume.

서식 지정함: 글꼴: 굵게, 글꼴 색: 텍스트 1
서식 지정함: 글꼴: 굵게, 글꼴 색: 텍스트 1
서식 있음: 왼쪽
서식 지정함: 글꼴: 굵게, 글꼴 색: 텍스트 1
서식 지정함: 글꼴 색: 텍스트 1
서식 지정함: 글꼴 색: 텍스트 1
서식 지정함: 글꼴 색: 텍스트 1
서식 지정함: 글꼴 색: 텍스트 1
서식 지정함: 글꼴 색: 텍스트 1
서식 지정함: 글꼴 색: 텍스트 1
서식 지정함: 글꼴 색: 텍스트 1
서식 지정함: 글꼴 색: 텍스트 1
서식 지정함: 글꼴: 굵게, 기울임꼴 없음, 글꼴 색: 텍스트 1
서식 지정함: 글꼴: 굵게, 기울임꼴 없음, 글꼴 색: 텍스트 1
서식 지정함: 글꼴 색: 텍스트 1

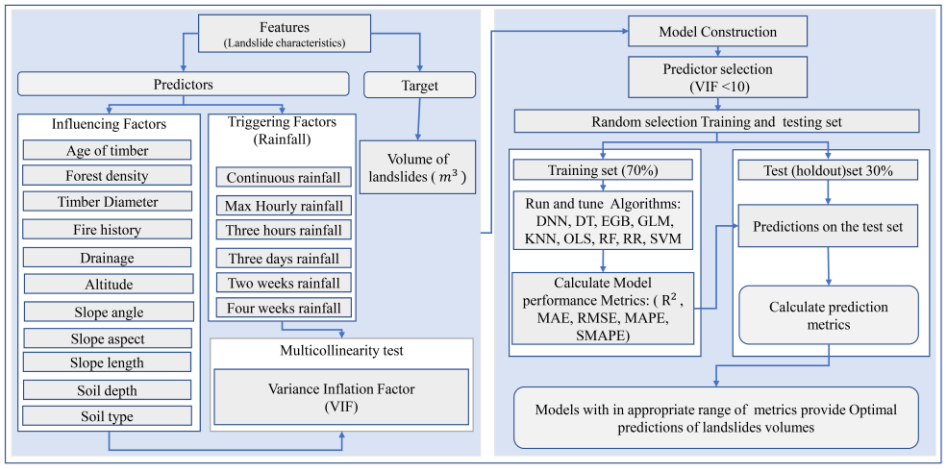

Figure 3. Workflow for the prediction of the volume of landslides due to rainfall.

3.1 Model Construction

In the present investigation, we aimed at predicting the volume of landslides using models that minimize error with interpretability and scalability. Since one model can not have all properties at the same time, we decided to select some of the models with those properties. The OLS, GLM, and DT were widely used for their high interpretability, which helps to understand the influence of individual features on predictions (Gelman, 2007; Breiman, 2017). On the other hand, the EGB, RF, SVM, RR, and KNN were used due to their robust performance in capturing complex patterns in data, which is essential for accurate predictions of landslide volumes (Chen and Guestrin, 2016; Liaw and Wiener, 2002; Hastie, 2009). Additionally, considering that the model will be used on a regional scale, which will require big data, the EGB, RF, and DNN are designed to efficiently handle large datasets, making them suitable for the regional scale analysis. These last models can be scaled to incorporate more data from different geographical areas without significant adjustments, enhancing their applicability in future research (Krizhevsky et al., 2012). Accordingly, nine data-driven methods were selected and tested on a Korean dataset to predict VLDR.

The first considered method is OLS, which is applied to estimate parameters of multilinear regression that yield the minimum residual sum of squares errors from the data (Dismuke and Lindrooth, 2006) under assumptions of no correlation in independent variables and in error term,

서식 지정함: 글꼴 색: 텍스트 1
서식 있음: 들여쓰기: 첫 줄: 1.27 cm
서식 지정함: 글꼴 색: 텍스트 1

constant variance in error terms, non-linear collinearity of predictors, and normal distribution of error terms. The RF-regression is a supervised data-driven technique based on ~~the~~ ensemble learning, which ~~construct~~constructs many decision trees during the training time of a model by combining multiple decision trees to produce an improved overall result of the model outcome. The RF-regression is more efficient in the analysis of multidimensional ~~dataset~~datasets (Borup et al., 2023). RF is an effective predictive model due to non-overfitting characteristics based on the law of large numbers (Breiman, 2001). The decision tree (DT) regression is a predictive modeling technique in ~~a~~the form of a flowchart-like tree structure ~~of~~that includes all possible results, output, predictor costs, and utility. The DT simplifies the decision-making due to its algorithm that mimic human brain decision-making patterns (Rathore and Kumar, 2016). The KNN technique draws an imaginary boundary in which prediction outcomes are allocated as the average of k-nearest point predictors and averaging their output variable (response). The KNN calculates Euclidian distances to identify likeness between datapoints and then it groups points that have smaller distances between them (Kramer and Kramer, 2013). The RR is an improved form of ordinary least square, which serves to respond to ~~the case~~cases where ~~the~~ collinearity is found in predictor variables. The estimated coefficients of ridge are biased estimators of true coefficients and are generated after adding a penalty on the OLS model. The RR has always lower variances compared to OLS (Saleh et al., 2019). The advantage of the GLM over OLS is that the dependent variable need not follow the normal distribution. The GLM is composed by random and systematic components, and the link function that links the two. In this study, the GLM with Gaussian link function was applied. GLM are fitted using maximum likelihood estimation (Dobson and Barnett, 2018). The DNN are among data-driven models that revolutionized different fields; the DNN learns via multi-processing layers and identifies intricate patterns in the data to predict the outcome (LeCun et al., 2015). Here, the backpropagation algorithm was used to predict the estimated outcome. The advantage of DNN is to discover the complex structures in the data using a back propagation algorithm with the capability to change the internal parameter (weight update). The SVM is popular for balanced predictive performance which makes it capable to train model on small sample size (Pisner and Schnyer, 2020). SVM has been applied in many different landslide studies (Pham et al., 2018; Miao et al., 2018). SVM methods identify the optimal hyperplane in ~~multi-dimensional~~multidimensional space that separates different groups in the output values. The EGB is the most powerful and leading supervised machine learning method in solving regression

서식 지정함: 글꼴 색: 텍스트 1

problems. It can perform parallel processing on ~~windows~~Windows, and Linux (Chen et al., ~~2015~~2015b). The gradient boosting trains of differentiable loss function, and the model fits when the gradient is minimized. In this paper, both traditional statistical predictive models and machine learning models were used. The firsts are known for high clarity and ~~explain ability~~explainability, and the second is famous for handling non-linearity in features. In some cases, the performance of advanced data-driven algorithms is almost similar (Chowdhury~~,~~ et al., 2023).

3.2 Feature selection and data splitting

The variable selection procedure was carried out based on previous literature and applied in the model using generalized variance inflation factor (GVIF) (O'Brien, 2007) to eliminate collinear variables. The variable with GVIF<10 was considered non-colinear and used in the model. Figure 4 depicts retained features and corresponding GVIF values. The retained features have GVIF less than 10 (O'brien, 2007). Accordingly, all depicted variables were considered for the model training. Further, to train the model, the datasets were split randomly, with 70% of the data for the training set and 30% for testing (Nguyen et al., 2021). The 10-fold cross-validation was performed to obtain an optimal model.

The training and test set was scaled (Z-score or variance stability scaling) to solve convergence issues that are associated with running the model without feature scaling (Singh and Singh, 2022). To run the model on the data using driven methods that accept numerical features only, the test and training set was one-hot-encoded to create a feature matrix (Seger, 2018).

서식 지정함: 글꼴 색: 텍스트 1

서식 지정함: 글꼴 색: 텍스트 1

서식 지정함: 글꼴 색: 텍스트 1

서식 지정함: 글꼴 색: 텍스트 1

서식 지정함: 글꼴 색: 텍스트 1

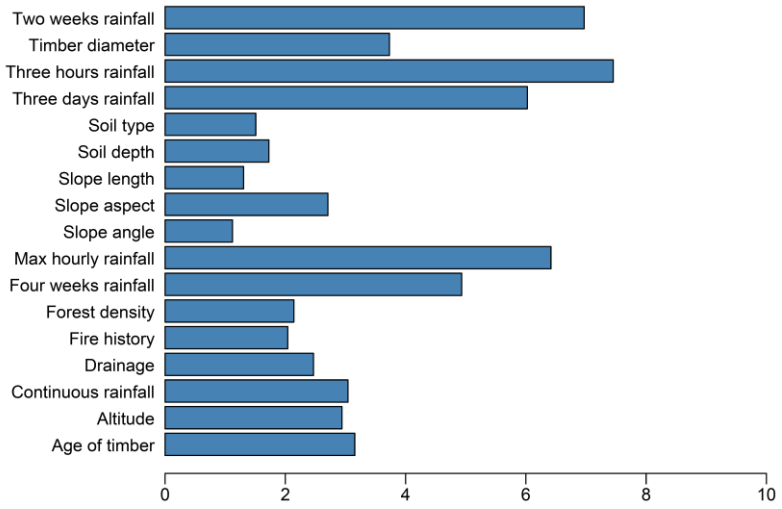

Figure 4. Generalized Variance Inflation Factor (GVIF) bar plot for features.

3.3 Model evaluation metrics

The model performance evaluation is a process of quantifying the difference between the observed value not used in the modeling process and the predicted value by the model. Different metrics are applied depending on the type of task, whether it is a classification or a regression problem. Subsequently, the widely used evaluation metrics for regression models, namely, R^2, MAE, RMSE, MAPE and SMAPE, were utilized to evaluate the model performances. The metric formulae and evaluation criteria are summarized in Table 3.

Table 3. Model evaluation metrics.

Metrics	Evaluation	Reference
$RMSE = \sqrt{\frac{1}{n}\sum_{i=1}^{n}(y_i - \hat{y}_i)^2}$	• Measures the square root of the average squared differences between predicted and actual values. • Lower values indicate better model performance.	Hyndman and Koehler, 2006.
$MAE = \frac{1}{n}\sum_{i=1}^{n}\lvert y_i - \hat{y}_i \rvert$	• The average of the absolute differences between predicted and actual values. • Lower values indicate better model performance.	Willmott and Matsuura, 2005

$MAPE = \frac{100}{n}\sum_{i=1}^{n}\left\|\frac{y_i - \hat{y}_i}{y_i}\right\|$	• Measures the accuracy of a model as a percentage, which can be more interpretable. • Lower values indicate better model performance.	Armstrong, 2001
$SMAPE = \frac{100}{n}\sum_{i=1}^{n}\frac{\|y_i - \hat{y}_i\|}{\|y_i\| - \|\widehat{y_i}\|}$	• Unlike MAPE, which can be skewed by very small actual values, SMAPE accounts for both the actual and predicted values, making it symmetric. • SMAPE is expressed as a percentage • Mitigates the impact of small actual values on the error metric, providing a more balanced assessment. • Lower values indicate better model performance.	Hyndman and Koehler, 2006
$R^2 = 1 - \frac{\sum_{i=1}^{n}(y_i - \hat{y}_i)^2}{\sum_{i=1}^{n}(y_i - \bar{y})^2}$	• Represents the proportion of variance in the dependent variable that can be explained by the independent variables. • Values closer to 1 indicate a better fit	Darlington, 1990; Chicco et al., 2021

*y_i and $\hat{y}_i$ representing the actual and predicted value and, $\bar{y}$ and n standing for the mean of actual value and number of observations in the dataset, respectively.

서식 지정함: 글꼴 색: 텍스트 1

서식 있음: 양쪽, 간격 단락 뒤: 0 pt, 단락의 첫 줄이나 마지막 줄 분리 허용, 단어 잘림 허용, 한글과 영어 간격을 자동으로 조절하지 않음, 한글과 숫자 간격을 자동으로 조절하지 않음

4. Results

~~Prior to the construction of the model, the collinearity analysis was performed and variable with less variance inflation factor were retained for training and testing models. Figure 3 depicts retained features and corresponding VIF values. The retained features have VIF less than 10 (O'brien, 2007). All predictors except three days rainfall exhibited VIF less than 5 and still less than 10. Accordingly, all depicted variables were considered for predictive model construction.~~

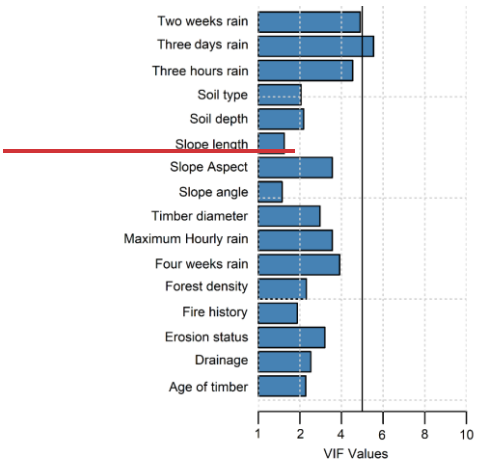

~~Figure 3. Variance inflation factor bar plot for explanatory variables.~~

The model was developed in R with different libraries, as discussed below. The DNN regression model was constructed using dnn() function from the cito library (Amesoeder et al., 2023), with ~~three~~two hidden layers of (50,~~50,~~ 50) nodes. ~~Model~~The model was trained on ~~208L~~1500L epochs, learning rate (lr = 0.~~1~~01), and loss = "mae". The decision tree regression model was constructed with tree() function from the tree library, with the recursive-partition method. The ridge regression model was constructed using glmnet() function from glmnet library~~(Jerome~~ (Friedman et al., 2010). ~~the~~The optimal lambda was obtained by performing 10-fold cross-validation. The EGB model was built using xgboost() function in xgboost ~~packagages~~package (Chen et al., 2022). The optimal model was obtained at ~~357th~~524th boosting iteration with ~~all~~max depth = 5 and other parameters set to default. The GLM regression model was constructed using glm() function~~(~~ (R core Team, 2022) with family ~~gaussian~~Gaussian and ~~identity~~log link~~.~~ to constrain the model of predicting positive outcomes. The KNN regression was constructed using knnreg() function from the caret package (Kuhn, 2022~~,~~), with number of neighbors ~~(, *k*=7).~~17. The OLS model was constructed lm() from the stats package (R core Team, 2022). The RF model was run using randomForest() from the randomforest package (Liaw and Wiener, 2002~~),~~) with default parameters and the optimal model was reached at ~~63rd~~256th iteration. The ridge regression model was constructed using glmnet() from the glmnet package (~~Jerome~~Friedman et al., ~~2012~~2010), with

서식 지정함: 글꼴 색: 텍스트 1
서식 지정함: 글꼴 색: 텍스트 1
서식 지정함: 글꼴 색: 텍스트 1
서식 지정함: 글꼴 색: 텍스트 1
서식 지정함: 글꼴 색: 텍스트 1
서식 지정함: 글꼴 색: 텍스트 1
서식 지정함: 글꼴 색: 텍스트 1
서식 지정함: 글꼴 색: 텍스트 1
서식 지정함: 글꼴 색: 텍스트 1
서식 지정함: 글꼴 색: 텍스트 1
서식 지정함: 글꼴 색: 텍스트 1
서식 지정함: 글꼴 색: 텍스트 1
서식 지정함: 글꼴 색: 텍스트 1
서식 지정함: 글꼴 색: 텍스트 1
서식 지정함: 글꼴 색: 텍스트 1
서식 지정함: 글꼴 색: 텍스트 1
서식 지정함: 글꼴 색: 텍스트 1
서식 지정함: 글꼴 색: 텍스트 1
서식 지정함: 글꼴 색: 텍스트 1
서식 지정함: 글꼴 색: 텍스트 1
서식 지정함: 글꼴 색: 텍스트 1
서식 지정함: 글꼴 색: 텍스트 1
서식 지정함: 글꼴: 기울임꼴, 글꼴 색: 텍스트 1
서식 지정함: 글꼴 색: 텍스트 1
서식 지정함: 글꼴 색: 텍스트 1
서식 지정함: 글꼴 색: 텍스트 1
서식 지정함: 글꼴 색: 텍스트 1
서식 지정함: 글꼴 색: 텍스트 1
서식 지정함: 글꼴 색: 텍스트 1
서식 지정함: 글꼴 색: 텍스트 1
서식 지정함: 글꼴 색: 텍스트 1
서식 지정함: 글꼴 색: 텍스트 1
서식 지정함: 글꼴 색: 텍스트 1

ridge penalty (alpha=0). The SVM regression model with linear kernel was built using e1071 package (Meyer et al., 2021) and other parameters set to default.

The predictive performance of all tested models ~~was summarized in~~ on the holdout dataset is depicted by the scatterplot (Fig. 4~~5~~) of actual volume as recorded in the test set and predicted outcome values of each model. The red line represents the perfect prediction. The scatter plot of actual and predicted values of tested models shows that OLS performed least compared to other models with R^2=0.~~27~~2744, that is, ~~27~~29% of ~~variance~~variances in the model ~~could be~~were explained by ~~predictor variables.~~predictors. The second least performing was ~~GLM~~the RR with R^2= 0.~~29 that~~3034, which is ~~23~~.6% improvement compared to OLS. Among all models ~~five~~, three out of nine, namely, OLS~~, KNN, GLM~~, SVM, and RR, performed below 50%; however, these models predicted well small values of volume (below 2000m^3). The MAE of these ~~five~~three models was higher than the remaining ~~four~~six models, namely DNN, DT, GLM, KNN, RF, ~~DNN~~ and EGB. Among these lasts, the most performing was EGB with R^2= 0.~~85~~88 of variance explained by predictors and MAE=~~245~~146.6 m^3. The ~~summary of coefficients of determination~~evaluation metrics for the training and ~~mean absolute errors for~~ tested models are summarized in Table ~~3.~~ 4. Considering the R^2, the three models, namely EGB, RF, and DNN, had a value of R^2 above 80% on the holdout set.

서식 지정함: 글꼴 색: 텍스트 1

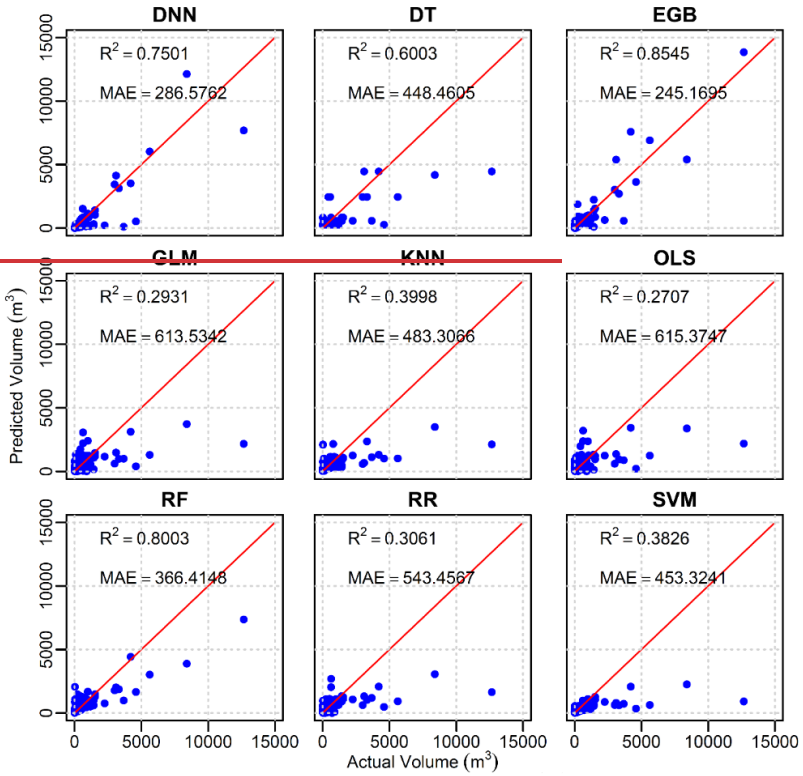
DNN
DT
EGB
GLM
KNN
OLS
RF
RR
SVM
R² = 0.7501
MAE = 286.5762
R² = 0.6003
MAE = 448.4605
R² = 0.8545
MAE = 245.1695
R² = 0.2931
MAE = 613.5342
R² = 0.3998
MAE = 483.3066
R² = 0.2707
MAE = 615.3747
R² = 0.8003
MAE = 366.4148
R² = 0.3061
MAE = 543.4567
R² = 0.3826
MAE = 453.3241
Predicted Volume (m³)
Actual Volume (m³)
0
5000
10000
15000

495

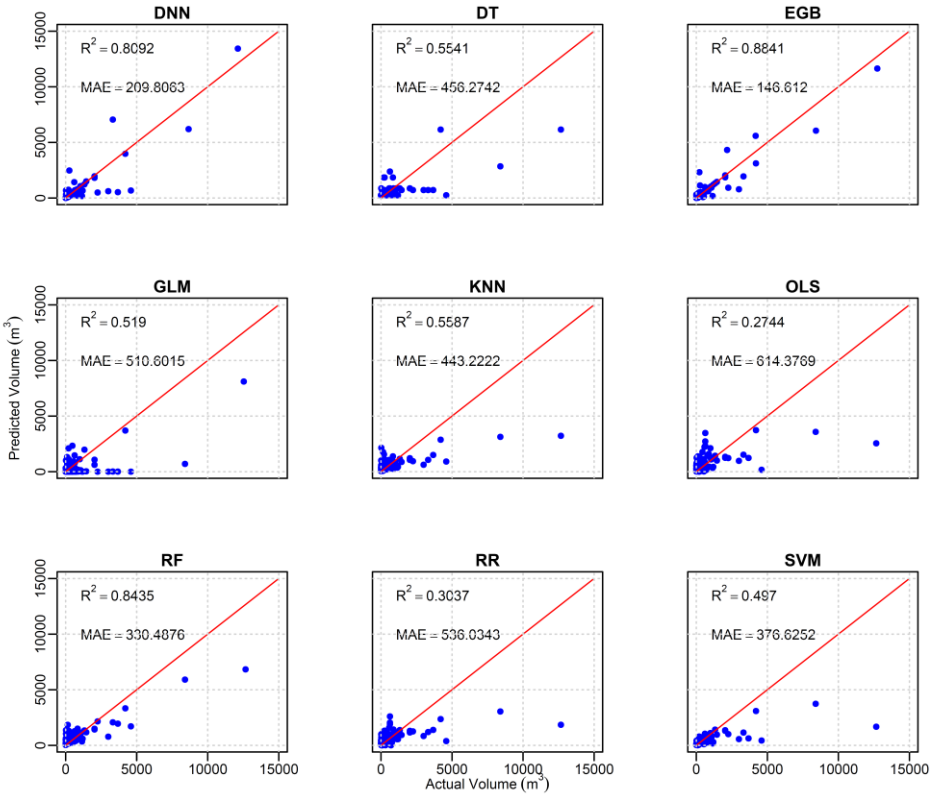

Figure 45. Scatterplot of actual and predicted values for nine tested models.

Regarding the prediction on the training set, the GLM had an R^2 of 83%. Nevertheless, the prediction on the holdout set was 51.9%; this large variation in variance explained by predictors indicates that the GLM model did not catch all non-linear patterns in the holdout set. It is noteworthy that the prediction difference in R^2 on both training and test for the random forest exhibited a very small difference compared to EGB and DNN, that is, 1.75% compared to 12.17% and 7.72% for DNN and EGB, respectively. Despite the stable prediction of RF, the performance in terms of SMAPE, the DNN was the second lowest symmetric mean absolute percentage error, 43.83m^3 and 39.79 m^3 on training and test sets, respectively. According to Chicco et al. (2021), the R^2 is more informative in regression modeling; thus, RF had better predictions than the DNN.

서식 지정함: 글꼴 색: 텍스트 1

서식 지정함: 글꼴 색: 텍스트 1

서식 있음: 양쪽, 들여쓰기: 첫 줄: 0.16 cm, 간격 단락 뒤: 0 pt

서식 있음: 양쪽, 간격 단락 뒤: 0 pt

Table ~~3~~4. Summary of ~~R2 and MAE~~prediction metrics for tested models on the training and test set.

Metrics ~~Models~~		Models								
		DNN	DT	EGB	GLM	KNN	OLS	RF	RR	SVM
R2	Train	0.~~7501~~93 09	0.~~6003~~45 14	0.~~8545~~96 13	0.~~2931~~83 80	0.~~3998~~34 70	0.~~2707~~37 75	0.~~8003~~86 10	0.~~3061~~33 82	0.~~382~~ ~~6~~5510
	Test	0.8092	0.5822	0.8841	0.5190	0.5587	0.2744	0.8435	0.3037	0.4970
MAE	~~286.57~~ ~~62~~Train	~~448.4605~~ 132.7429	~~245.1695~~ 407.0814	~~613.534~~ ~~2~~75.1250	~~483.3066~~ 308.9700	~~615.3747~~ 410.2945	~~366.4148~~ 502.0053	~~543.4567~~ 236.9516	~~453.3241~~ 470.1633	276.20 00
	Test	209.8063	435.5836	146.6120	510.6015	443.2222	614.3769	330.4876	536.0343	376.62 52
RMSE	Train	348.6190	940.4850	113.4940	570.0070	1027.3730	1001.7620	574.9720	1042.9110	916.54 71
	Test	646.5438	1047.4880	501.8960	1055.9190	1115.5270	1234.1220	737.0857	1237.9420	1176.9 410
MAPE	Train	0.5240	0.7930	0.1540	76.3530	0.6280	5.2310	0.3810	1.5330	1.1588
	Test	0.5623	0.8892	0.3132	1819.2220	0.6623	4.1277	0.4939	5.8428	1.0421
SMAPE	Train	43.8375	79.8680	13.1780	150.4262	67.4715	103.0555	52.3359	93.4002	67.322 1
	Test	39.7998	81.4539	22.7237	152.4991	73.6498	106.9756	63.7582	93.9244	76.979 4

To dive deep into the prediction performance of the EGB model, we analyzed variables importance in the prediction of the volume. It was observed that ~~the~~ slope length was the most contributing predictor in the performance of the EGB model, followed by ~~the~~ maximum hourly rainfall and slope aspect. The ~~presence~~altitude, three hours rainfall, slope angle and ~~quality~~age of ~~drainage ranked the third most contributor~~timber contributed moderately in the prediction of the ~~volume of rainfall due~~outcome volumes with gain above 0.01 and less than 0.2. the antecedent rainfall from three days and above and continuous rainfall had a minor contribution, with a gain of less than 0.01 for each. The presence of rainwater drainage channels had a moderate contribution, with a gain close to ~~landslides. In addition, age of timber (age~~0.01. On the other hand, the contribution of ~~trees~~soil depth and forest density in the models was insignificant and far below 0.01. Though Figure 2(g) depicted the association between larger volumes and fire history, the variable importance indicates that ~~were planted~~the relation was not significant. Even though some variables had minor contributions, depending on the ~~area that faced landslides) and maximum hourly rainfall have~~case, the contribution of those variables may also ~~shown a significant contribution in the prediction of volume of landslide due to rainfall. Figure 5~~increase depending on other regional settings. Therefore, all variables with Generalized variance inflation factors below 10 were kept in the model. Figure 6 illustrates ~~a list of independent variables that had a~~

서식 지정함
서식 있음: 줄 간격: 1줄
서식 지정함: 글꼴: 8 pt, 글꼴 색: 텍스트 1
서식 있음: 줄 간격: 1줄
삽입한 셀
서식 지정함: 글꼴: Calibri, 8 pt, 글꼴 색: 텍스트 1
서식 지정함: 글꼴: 8 pt, 글꼴 색: 텍스트 1
서식 있음: 줄 간격: 1줄
병합한 셀
서식 지정함: 글꼴: 8 pt, 글꼴 색: 텍스트 1
서식 있음: 가운데, 줄 간격: 1줄
서식 지정함: 글꼴: 8 pt, 글꼴 색: 텍스트 1
서식 지정함: 글꼴: 8 pt, 글꼴 색: 텍스트 1
서식 지정함: 글꼴: 8 pt, 글꼴 색: 텍스트 1
서식 지정함: 글꼴: 8 pt, 글꼴 색: 텍스트 1
서식 지정함: 글꼴: 8 pt, 글꼴 색: 텍스트 1
서식 지정함: 글꼴: 8 pt, 글꼴 색: 텍스트 1
서식 지정함: 글꼴: 8 pt, 글꼴 색: 텍스트 1
서식 지정함: 글꼴: 8 pt, 글꼴 색: 텍스트 1
서식 지정함: 글꼴: 8 pt, 글꼴 색: 텍스트 1
서식 있음: 왼쪽, 줄 간격: 1줄
서식 있음: 줄 간격: 1줄
삽입한 셀
서식 지정함: 글꼴: 8 pt, 글꼴 색: 텍스트 1
서식 있음: 가운데, 줄 간격: 1줄
서식 지정함: 글꼴: 8 pt, 글꼴 색: 텍스트 1
서식 지정함: 글꼴: 8 pt, 글꼴 색: 텍스트 1
서식 지정함: 글꼴: 8 pt, 글꼴 색: 텍스트 1
서식 지정함: 글꼴: 8 pt, 글꼴 색: 텍스트 1
서식 지정함: 글꼴: 8 pt, 글꼴 색: 텍스트 1
서식 지정함: 글꼴: 8 pt, 글꼴 색: 텍스트 1
서식 지정함: 글꼴: 8 pt, 글꼴 색: 텍스트 1
서식 지정함: 글꼴: 8 pt, 글꼴 색: 텍스트 1
서식 지정함: 글꼴: 8 pt, 글꼴 색: 텍스트 1
서식 지정함: 글꼴 색: 텍스트 1
서식 있음
서식 지정함

~~significant impact in the prediction of the volume~~the variables importance for the EGB model. The vertical red line split the variables into two groups, the first containing variables that contributed a gain above 0.01 and others with minor contributions.

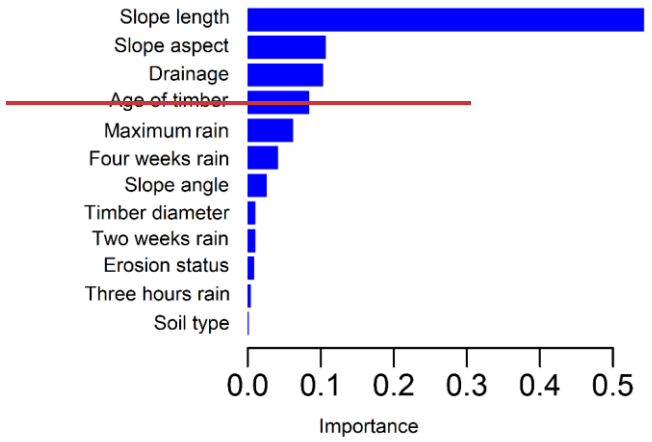

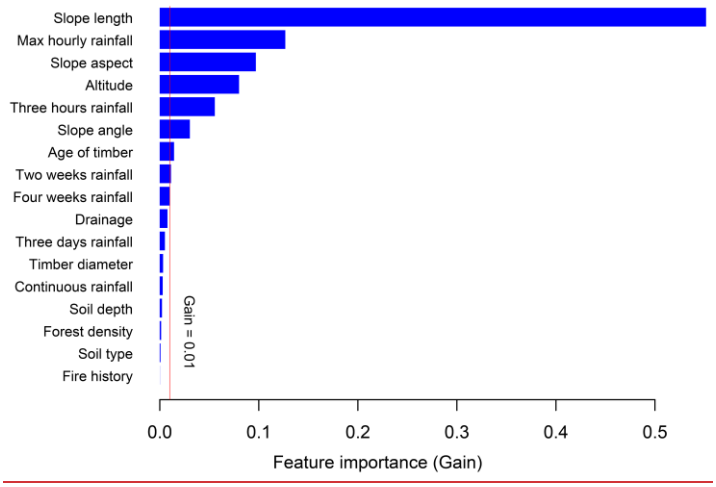

Figure ~~5~~6. Variable importance for the EGB model.

The variable importance plot depicts the overall contribution of a given variable; however, it does not provide detailed information. To get more insight into the relationship between the volume of landslides and predictors, statistical tests for normality, namely, Shapiro-Wilk's test,

서식 지정함: 글꼴 색: 텍스트 1

서식 지정함: 글꼴 색: 텍스트 1

서식 지정함: 글꼴 색: 텍스트 1

서식 지정함: 글꼴 색: 텍스트 1

~~Kruskal-Wallis test,~~ and Dunn's test were conducted. The Shapiro-Wilk's test (Dudley, 2023) results revealed that the distribution of volume was non-normal (W = 0.40642, p-value < 0.001).

Noting that the volume distribution was non-normal, we opted for the non-parametric tests, which do not rely on normality to conduct the distance correlation (Székely et al., 2007) test (dcor) for continuous independent features. Figure ~~6~~7 illustrates that the slope length exhibited a higher value (dcor=0.~~5~~156) followed by continuous rainfall ~~features. This highlights the role of current~~altitude and ~~antecedent~~three hours rainfall ~~as triggering factor in~~and kept decreasing up to timber diameter with a distance correlation of 0.08. Overall, the distance correlation between the ~~prediction of~~ volume of landslides shows a moderate strength of association between continuous predictors.

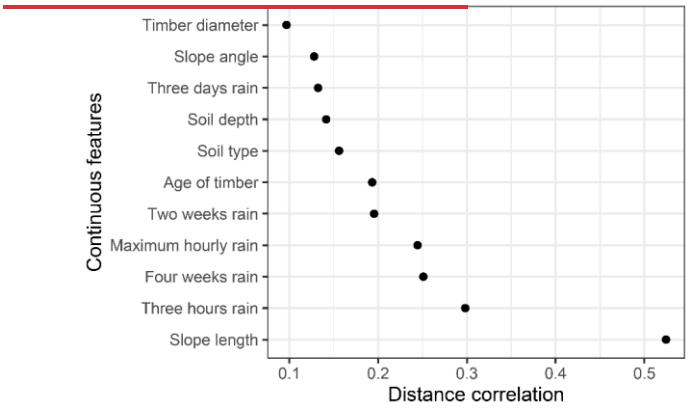

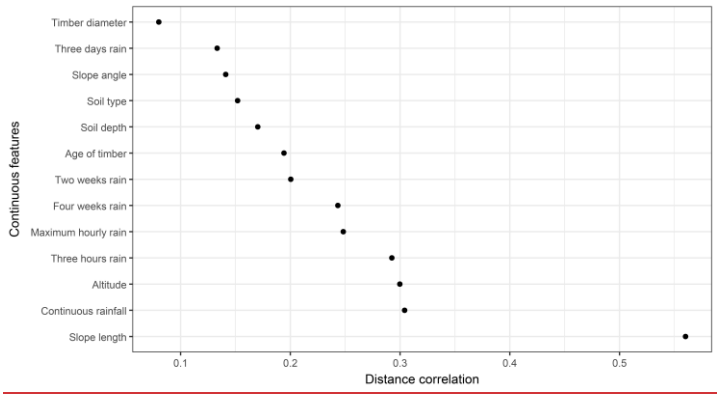

서식 지정함: 글꼴 색: 텍스트 1
서식 지정함: 글꼴 색: 텍스트 1
서식 지정함: 글꼴 색: 텍스트 1
서식 있음: 들여쓰기: 첫 줄: 1.27 cm
서식 지정함: 글꼴 색: 텍스트 1
서식 지정함: 글꼴 색: 텍스트 1
서식 지정함: 글꼴 색: 텍스트 1
서식 지정함: 글꼴 색: 텍스트 1
서식 지정함: 글꼴 색: 텍스트 1
서식 지정함: 글꼴 색: 텍스트 1
서식 지정함: 글꼴 색: 텍스트 1
서식 지정함: 글꼴 색: 텍스트 1
서식 지정함: 글꼴 색: 텍스트 1

Figure ~~6~~7. Distance correlation plot for the volume and continuous features.

Furthermore, to test for categorical features, Kruskal-Wallis test (McKight and Najab, 2010) was used to check whether the volume of the landslide was different in each category and Dunn's tests (Dinno, 2015) were applied to examine which categories had similar means of the volume of landslides due to rainfall in different categories. The H_0 (null hypothesis) was that the mean volume of landslides in different categories is the same, and the H_1 (alternative hypothesis) was that the means of landsides are different in some categories. For the slope aspect, the second most significant predictor for the EGB model, the results of Kruskal-Wallis test (chi-squared = 20.889, df = 7, p-value = 0.003938) showed that there is a significant difference in median of volume in some categories of slope aspects. To know which classes of slope aspects had significantly different mean volumes, the Dunn's test results at 95% confidence interval, pairs (East-South west, East-South East, East-South, East-North West and North West-South East) had significantly different means of landslides' volume (with p-value <0.05). Figure ~~7~~8 depicts that the southwest and southeast aspects had a higher frequency of landslides.

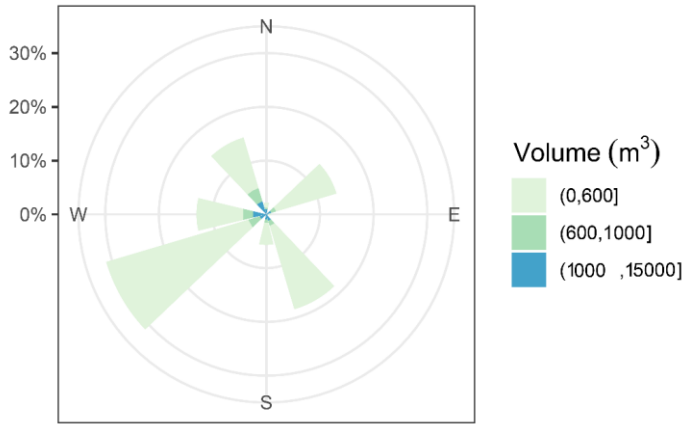

Figure ~~7~~8. The distribution of the volume of landslides due to rainfall with respect to the slope aspect.

The Kruskal-Wallis test for the difference in mean of drainage classes showed the result was: chi-squared = 15.792, df = 2, p-value = 0.000372, which shows that the means of volume per ~~classes~~class were different. This was clarified by Dunn's test results, were p-values were less than

서식 지정함: 글꼴 색: 텍스트 1
서식 지정함: 글꼴 색: 텍스트 1
서식 지정함: 글꼴 색: 텍스트 1
서식 지정함: 글꼴 색: 텍스트 1
서식 지정함: 글꼴 색: 텍스트 1
서식 지정함: 글꼴 색: 텍스트 1
서식 지정함: 글꼴 색: 텍스트 1
서식 지정함: 글꼴 색: 텍스트 1
서식 있음: 들여쓰기: 왼쪽: 0 cm, 내어쓰기: 9.9 글자, 줄 간격: 배수 1.15 줄
서식 지정함: 글꼴 색: 텍스트 1
서식 지정함: 글꼴 색: 텍스트 1
서식 지정함: 글꼴 색: 텍스트 1
서식 지정함: 글꼴 색: 텍스트 1

0.05 in all pairwise mean difference comparisons. The results of these tests highlighted that ~~the~~ drainage has a remarkable influence on the occurrence of rainfall-induced landslides in the Korean Peninsula.

5. Discussion

This study aim was to construct ~~data~~a data-driven algorithm that ~~predict~~predicts the volume of ~~landslide~~landslides due to rainfall. The result of nine different tested algorithms revealed a tremendous difference between classical regression models (OLS, RR, and GLM) and other data -driven machine learning models. In this study, apart from SVM regression, DT and KNN, other machine learning models (DNN, DT, RF, and EGB) exhibited high prediction capability with R^2 above 50% (Fig.~~3~~5). The random forest~~,~~ model performed well in predicting smaller volume however as the volume increased the model underpredicted volume values. The DNN model performed quite well with low MAE ~~compare~~compared to random forest; however, the model did not perform ~~on~~ well on moderate volume values ~~which resulted~~, resulting in ~~reduction of~~reduced R^2. The EGB model tested on South Korean landslide inventory coupled with rainfall data at the time of landslide events and antecedent rainfall within one month of the event exhibited the highest performance compared to other constructed algorithms. The difference in performance may be due to the internal structure of each algorithm; the RF build multiple decision trees and averages predictions to improve accuracy (Breiman, 2001), while the EGB builds sequential trees in a recursive order where the new built tree improves error occurred while building the previous decision tree and optimizes the loss function through a gradient descent (Chen and Guestrin, 2016).

The slope aspect played an important role in the prediction of the volume, and the landslide mostly occurred ~~on location~~in locations oriented toward south ~~west~~ southwest and ~~south east~~southeast. That may be due to the direction taken by ~~typhoon~~typhoons, which hit the ~~south west~~southwest versants of mountains upon landfall on the Korean peninsula toward the North East Pacific (Ha, 2022~~,~~; Lee et al., 2013). The findings of this research are congruent with those of Lee et al. (2013~~)~~), who also highlighted that the mountain versant oriented to strong wind direction may face more landslides. The study also highlighted that ~~the efficacy of~~a moderate rainwater drainage channel plays an important role in the prevention of landslides ~~which~~ due to ~~the~~its stabilizing effect. The landslide location and pattern follow the rainfall climate scenario, which highlighted a higher intensity of rainfall in the northeastern region of South Korea (Lee, 2016).

서식 지정함: 글꼴 색: 텍스트 1

The findings of this study are congruent with Zhang et al. (2019) observations that highlighted the low influence of soil type in landslide modeling and the maximum rainfall and cumulative three hours of rainfall were the most contributing rainfall, which indicated that these shallow landslides may have been triggered by sudden rainfall concentrated in few hours before the occurrence of the event. The occurrence of landslides triggered by rainfall is a complex phenomenon ~~which involve~~that involves many interrelated environmental ~~setting~~settings, human activity, geological conditions and climatic conditions. Moreover, the occurrence of typhoons is known to aggravate the landslides impacts on communities (Chang et al., 2008~~),~~); incorporating typhoon variables in future studies to customize for regional ~~setting~~settings may improve the accuracy of the model. The advantage of his research is that the constructed model has high predictive accuracy and can handle the non-linearity of predisposing factors. The model came to fill the gap of few literatures related to the prediction of the volume of landslides using data-driven techniques. This model can be a ~~better~~good tool to help policy makers to integrate the landslides volume risks in in policy to protect infrastructure and inhabitants dwelling near foot of mountains with high risks of being buried by geological materials resulting from landslides.

To understand the applicability of the developed models, the trained model was tested using unknown data (test data), with volume predictions generated solely based on the predictor variables; actual volume values were utilized only for evaluating model performance. We found that the DNN, EGB, GLM, and RF models achieved R^2>0.8, indicating that the model could yield reliable volume estimates in adjacent areas with similar geological and environmental conditions. It is also noted that the EGB, RF, and DNN are designed to efficiently handle large datasets, making them suitable for regional-scale analysis with high scalability. Thus, these models can be scaled to incorporate more data from different geographical areas without significant adjustments, enhancing their applicability in future research (Krizhevsky et al., 2012). Subsequently, the optimized model can aid in disaster risk management by providing timely information for early warning systems. Additionally, the insights gained from the model can inform land-use planning and policy decisions, allowing stakeholders to identify high-risk areas and implement mitigation strategies effectively. By integrating the model into existing monitoring frameworks, agencies can enhance their response capabilities and better allocate resources during heavy rainfall events.

The major limitation of this study is that the analysis is solely focused on shallow-seated landslides, specifically translational slope failures with volumes below 13,000m^3. Thus, the

서식 지정함: 글꼴 색: 텍스트 1
서식 지정함: 글꼴 색: 텍스트 1
서식 지정함: 글꼴 색: 텍스트 1
서식 지정함: 글꼴 색: 텍스트 1
서식 지정함: 글꼴 색: 텍스트 1
서식 지정함: 글꼴 색: 텍스트 1
서식 지정함: 글꼴 색: 텍스트 1

analysis may not fully capture the variability in landslide characteristics across different geomorphological and geological contexts. Deep-seated landslides, for instance, often exhibit distinct failure mechanisms, material compositions, and depositional patterns that influence their volumetric characteristics, which were not considered in this investigation. Similarly, debris flows, known for their unique channelization and entrainment behaviors, were not included, potentially limiting the applicability of the optimized models to other landslide types. Further, this study was also performed using point-based landslide inventory data, which may not capture all variability of influencing factors and their exact state. The incorporation of high-resolution data from remote sensing and other sources may also improve the efficiency of the predictions. These limitations may impact the broader applicability of the proposed model; however, future studies will aim to address this by conducting separate analyses for deep-seated landslides and debris flows, allowing for a more comprehensive understanding of landslide volume predictions across diverse landslide types and geomorphological settings.

6. Conclusions

In this paper, the aim was to construct ~~the~~a data ~~-~~driven model that ~~predict~~predicts the volume of landslides due to rainfall. To this, nine different classical regression models and machine learning algorithms were tested on South Korean landslide data set containing features of landslides that occurred between 2011 and 2012. Among the tested models, ~~Extreme~~extreme gradient boosting (EGB) produced the most accurate prediction. This is proven by the evaluation of the difference between actual and predicted values ~~were~~, such as R^2 ~~was 0.8545,~~= 88.41% and MAE ~~was 245.1695m^3,~~=146.6120m^3 on the test set. The analysis of feature variables in the contribution to the prediction of the model ~~-~~ revealed that the slope length was the most influencing predictor. The EGB model can be a promising tool for the prediction of the volume of ~~landslide~~landslides due to its high predictive performance. The model can be customized ~~on~~in different environmental settings. The model can be applied to estimate the expected volume of landslides based on forecasted rainfall once the model is well-adjusted to fit the geomorphological and environmental settings of the region of interest ~~-~~ after re-training on the regional historical data to include regional variability. Therefore, this model can be a ~~better~~good tool for planning for resilience and infrastructure pre-construction risk assessment to ensure the new infrastructure is placed in stable regions free from severe landslides.

서식 지정함: 글꼴 색: 텍스트 1

서식 지정함: 글꼴 색: 텍스트 1

서식 지정함: 글꼴 색: 텍스트 1

서식 지정함: 글꼴 색: 텍스트 1

서식 지정함: 글꼴 색: 텍스트 1

서식 지정함: 글꼴 색: 텍스트 1

서식 지정함: 글꼴 색: 텍스트 1

서식 지정함: 글꼴 색: 텍스트 1

서식 지정함: 글꼴 색: 텍스트 1

서식 지정함: 글꼴 색: 텍스트 1

서식 지정함: 글꼴 색: 텍스트 1

서식 지정함: 글꼴 색: 텍스트 1

Acknowledgments

This research was supported by through the National Research Foundation of Korea (NRF) funded by the Ministry of Education and Ministry of Science and ICT (2021R1A6A1A03044326, 2021R1C1C2003316). The authors highly appreciate both anonymous reviewers for their constructive suggestions that helped us improve the earlier preprint version.

Reference

Alcantara, A. L., and Ahn, K. H. (2020). Probability distribution and characterization of daily precipitation related to tropical cyclones over the Korean Peninsula. Water, 12(4), 1214.

Alcántara-Ayala, I. (2021). Integrated landslide disaster risk management (ILDRiM): the challenge to avoid the construction of new disaster risk. Environmental Hazards, 20(3), 323-344.

Alcántara-Ayala, I., & Sassa, K. (2023). Landslide risk management: from hazard to disaster risk reduction. Landslides, 20(10), 2031-2037.

Amatya, S. C. (2016). Landslide disaster management in Nepal: a near-future perspective. Nepal-Japan Friendship Association of Water Induced Disaster (NFAD), Japan Department of Water Induced Disaster Management (DWIDM).

Amesoeder, C., Hartig, F., and Pichler, M. (2023). cito: An R package for training neural networks using torch. arXiv e-prints, arXiv-2303.

Armstrong, J. S. (2001). Combining forecasts (pp. 417-439). Springer US.

Asada, H., & Minagawa, T. (2023). Impact of vegetation differences on shallow landslides: a case study in Aso, Japan. Water, 15(18), 3193.

Barik, M. G., Adam, J. C., Barber, M. E., & Muhunthan, B. (2017). Improved landslide susceptibility prediction for sustainable forest management in an altered climate. Engineering geology, 230, 104-117.

Bernardie, S., Desramaut, N., Malet, J.-P., Gourlay, M., and Grandjean, G. (2014). Prediction of changes in landslide rates induced by rainfall. Landslides, 12(3), 481–494. doi:10.1007/s10346-014-0495-8

Bonamutial, M., and Prasetyo, S. Y. (2023, August). Exploring the Impact of Feature Data Normalization and Standardization on Regression Models for Smartphone Price Prediction. In 2023 International Conference on Information Management and Technology (ICIMTech) (pp. 294-298). IEEE.

Borup, D., Christensen, B. J., Mühlbach, N. S., and Nielsen, M. S. (2023). Targeting predictors in random forest regression. International Journal of Forecasting, 39(2), 841-868.

Breiman, L. (2001). Random forests. Machine learning, 45, 5-32.

Breiman, L. (2017). Classification and regression trees. Routledge.

서식 지정함: 글꼴: 굵게, 글꼴 색: 텍스트 1, 영어(영국), 글자 커닝16 pt

서식 지정함: 글꼴 색: 텍스트 1

서식 지정함: 글꼴: 굵게 없음, 글꼴 색: 텍스트 1, 영어(미국)

서식 있음: 표준, 양쪽, 오른쪽: 0 cm, 간격 앞: 0 pt, 단락 뒤: 0 pt, 같은 스타일의 단락 사이에 공백 삽입, 단락의 첫 줄이나 마지막 줄 분리 허용, 단어 잘림 허용, 한글과 영어 간격을 자동으로 조절하지 않음, 한글과 숫자 간격을 자동으로 조절하지 않음

서식 지정함: 글꼴 색: 텍스트 1

서식 있음: 간격 단락 뒤: 0 pt, 줄 간격: 배수 1.15 줄, 금칙 처리 안 함, 문장 부호 끌어 맞추지 않음, 한글과 영어 간격을 자동으로 조절하지 않음, 한글과 숫자 간격을 자동으로 조절하지 않음

서식 지정함: 글꼴 색: 텍스트 1

서식 있음: 간격 단락 뒤: 0 pt, 줄 간격: 배수 1.15 줄, 금칙 처리 안 함, 문장 부호 끌어 맞추지 않음, 한글과 영어 간격을 자동으로 조절하지 않음, 한글과 숫자 간격을 자동으로 조절하지 않음

서식 지정함: 글꼴 색: 텍스트 1

서식 지정함: 글꼴 색: 텍스트 1

서식 지정함: 글꼴 색: 텍스트 1

서식 있음: 간격 단락 뒤: 0 pt, 줄 간격: 배수 1.15 줄, 금칙 처리 안 함, 문장 부호 끌어 맞추지 않음, 한글과 영어 간격을 자동으로 조절하지 않음, 한글과 숫자 간격을 자동으로 조절하지 않음

Cellek, S. (2021). The effect of aspect on landslide and its relationship with other parameters. In Landslides. IntechOpen.

Chang, K. T., and Chiang, S. H. (2009). An integrated model for predicting rainfall-induced landslides. Geomorphology, 105(3-4), 366-373.

Chang, K. T., Chiang, S. H., and Lei, F. (2008). Analysing the relationship between typhoon-triggered landslides and critical rainfall conditions. Earth Surface Processes and Landforms: The Journal of the British Geomorphological Research Group, 33(8), 1261-1271

Chatra, A. S., Dodagoudar, G. R., & Maji, V. B. (2019). Numerical modelling of rainfall effects on the stability of soil slopes. International Journal of Geotechnical Engineering.

Chen T, He T, Benesty M, Khotilovich V, Tang Y, Cho H, Chen K, Mitchell R, Cano I, Zhou T, Li M, Xie J, Lin M, Geng Y, Li Y, Yuan J (2022). _xgboost: Extreme Gradient Boosting_. R package version 1.6.0.1, <https://CRAN.R-project.org/package=xgboost>.

Chen, C. W., Oguchi, T., Hayakawa, Y. S., Saito, H., and Chen, H. (2017). Relationship between landslide size and rainfall conditions in Taiwan. Landslides, 14, 1235-1240.

Chen, L., Guo, Z., Yin, K., Shrestha, D. P., & Jin, S. (2019). The influence of land use and land cover change on landslide susceptibility: a case study in Zhushan Town, Xuan'en County (Hubei, China). Natural hazards and earth system sciences, 19(10), 2207-2228~~T., He, T., Benesty, M., Khotilovich, V., Tang, Y., Cho, H., ... and Zhou, T. (2015). Xgboost: extreme gradient boosting. R package version 0.4-2, 1(4), 1-4~~.

Chen, T., & Guestrin, C. (2016). Xgboost: A scalable tree boosting system. In Proceedings of the 22nd acm sigkdd international conference on knowledge discovery and data mining (pp. 785-794). <doi:10.1145/2939672.2939785>

Chen, Z., Luo, R., Huang, Z., Tu, W., Chen, J., Li, W., ... and Ai, Y. (~~2015~~2015a). Effects of different backfill soils on artificial soil quality for cut slope revegetation: Soil structure, soil erosion, moisture retention and soil C stock. Ecological engineering, 83, 5-12.

Chen, T., He, T., Benesty, M., Khotilovich, V., Tang, Y., Cho, H., ... and Zhou, T. (2015b). Xgboost: extreme gradient boosting. R package version 0.4-2, 1(4), 1-4.

Chen, X., Zhang, L., Zhang, L., Zhou, Y., Ye, G., & Guo, N. (2021). Modelling rainfall-induced landslides from initiation of instability to post-failure. Computers and geotechnics, 129, 103877.

Cheung, R. W. (2021). Landslide risk management in Hong Kong. Landslides, 18(10), 3457-3473.

Chicco, D., Warrens, M. J., & Jurman, G. (2021). The coefficient of determination R-squared is more informative than SMAPE, MAE, MAPE, MSE and RMSE in regression analysis evaluation. Peerj computer science, 7, e623.

Chowdhury, M. Z. I., Leung, A. A., Walker, R. L., Sikdar, K. C., O'Beirne, M., Quan, H., and Turin, T. C. (2023). A comparison of machine learning algorithms and traditional regression-based statistical modeling for predicting hypertension incidence in a Canadian population. Scientific Reports, 13(1), 13.

서식 지정함: 글꼴 색: 텍스트 1

서식 있음: 간격 단락 뒤: 0 pt, 줄 간격: 배수 1.15 줄, 금칙 처리 안 함, 문장 부호 끝어 맞추지 않음, 한글과 영어 간격을 자동으로 조절하지 않음, 한글과 숫자 간격을 자동으로 조절하지 않음

서식 지정함: 글꼴 색: 텍스트 1, 프랑스어(프랑스)

서식 지정함: 글꼴 색: 텍스트 1

서식 있음: 간격 단락 뒤: 0 pt, 줄 간격: 배수 1.15 줄, 금칙 처리 안 함, 문장 부호 끝어 맞추지 않음, 한글과 영어 간격을 자동으로 조절하지 않음, 한글과 숫자 간격을 자동으로 조절하지 않음

서식 지정함: 글꼴 색: 텍스트 1

서식 지정함: 글꼴 색: 텍스트 1

서식 지정함: 글꼴 색: 텍스트 1

서식 지정함: 글꼴 색: 텍스트 1

서식 있음: 간격 단락 뒤: 0 pt, 줄 간격: 배수 1.15 줄, 금칙 처리 안 함, 문장 부호 끝어 맞추지 않음, 한글과 영어 간격을 자동으로 조절하지 않음, 한글과 숫자 간격을 자동으로 조절하지 않음, 탭: 4.5 글자, 왼쪽

서식 지정함: 글꼴 색: 텍스트 1

서식 지정함: 글꼴 색: 텍스트 1

서식 지정함: 글꼴 색: 텍스트 1

서식 있음: 간격 단락 뒤: 0 pt, 줄 간격: 배수 1.15 줄, 금칙 처리 안 함, 문장 부호 끝어 맞추지 않음, 한글과 영어 간격을 자동으로 조절하지 않음, 한글과 숫자 간격을 자동으로 조절하지 않음

Cohen, D., & Schwarz, M. (2017). Tree-root control of shallow landslides. Earth Surface Dynamics, 5(3), 451-477.

Conte, E., Pugliese, L., and Troncone, A. (2022). A simple method for predicting rainfall-induced shallow landslides. Journal of Geotechnical and Geoenvironmental Engineering, 148(10), 04022079

Culler, E. S., Livneh, B., Rajagopalan, B., ~~and~~& Tiampo, K. F. (2021). A data-driven evaluation of post-fire landslide susceptibility. Natural Hazards and Earth System Sciences Discussions, ~~1-24.~~2021, 1-24. https://doi.org/10.5194/nhess-23-1631-2023

Dai, F. C., ~~and~~& Lee, C. F. (2001). Frequency–volume relation and prediction of rainfall-induced landslides. Engineering geology, 59(3-4), 253-266.

Dai, F. C., Lee, C., F., & Ngai, Y. Y. (2002). Landslide risk assessment and management: an overview. Engineering geology, 64(1), 65-87.

Dai, K., Xu, Q., Li, Z., Tomás, R., Fan, X., Dong, X., ... and Ran, P. (2019). Post-disaster assessment of 2017 catastrophic Xinmo landslide (China) by spaceborne SAR interferometry. Landslides, 16, 1189-1199.

Darlington, R. B. (1990). Regression and linear models. Mcgraw-Hill College.

Dikshit, A., Satyam, N., & Pradhan, B., 2019. Estimation of rainfall-induced landslides using the TRIGRS model. Earth Systems and Environment, 3, 575-584.

Dinno, A. (2015). Nonparametric pairwise multiple comparisons in independent groups using Dunn's test. The Stata Journal, 15(1), 292-300.

Dismuke, C., and Lindrooth, R. (2006). Ordinary least squares. Methods and designs for outcomes research, 93(1), 93-104.

Dobson, A. J., and Barnett, A. G. (2018). An introduction to generalized linear models. CRC press

Donnarumma, A., Revellino, P., Grelle, G., and Guadagno, F. M. (2013). Slope angle as indicator parameter of landslide susceptibility in a geologically complex area. Landslide Science and Practice: Volume 1: Landslide Inventory and Susceptibility and Hazard Zoning, 425-433.

Duc, D. M. (2013). Rainfall-triggered large landslides on 15 December 2005 in Van Canh district, Binh Dinh province, Vietnam. Landslides, 10(2), 219-230.

Dudley, R. (2023). The Shapiro–Wilk test for normality. Available at https://math.mit.edu/~rmd/46512/shapiro.pdf

Evans, S. G., Mugnozza, G. S., Strom, A., and Hermanns, R. L. (Eds.). (2007). Landslides from massive rock slope failure (Vol. 49). Springer Science and Business Media.

Fan, ~~J. R., Zhang, X. Y., Su, F. H., Ge, Y.~~ X., Xu, Q., Liu, J., Subramanian, S. S., He, C., Zhu, X., & Zhou, L. (2019). Successful early warning and emergency response of a disastrous rockslide in Guizhou province, China. Landslides, 16, 2445-2457~~G., Tarolli, P., Yang, Z. Y., ... and Zeng, Z. (2017). Geometrical feature analysis and disaster assessment of the Xinmo landslide based on remote sensing data. Journal of Mountain Science, 14(9), 1677-1688~~.

서식 지정함: 글꼴 색: 텍스트 1

서식 있음: 간격 단락 뒤: 0 pt, 줄 간격: 배수 1.15 줄, 금칙 처리 안 함, 문장 부호 끝어 맞추지 않음, 한글과 영어 간격을 자동으로 조절하지 않음, 한글과 숫자 간격을 자동으로 조절하지 않음

서식 지정함: 글꼴 색: 텍스트 1

서식 지정함: 글꼴 색: 텍스트 1

서식 지정함: 글꼴 색: 텍스트 1

서식 지정함: 글꼴 색: 텍스트 1

서식 지정함: 글꼴 색: 텍스트 1

서식 있음: 간격 단락 뒤: 0 pt, 줄 간격: 배수 1.15 줄, 금칙 처리 안 함, 문장 부호 끝어 맞추지 않음, 한글과 영어 간격을 자동으로 조절하지 않음, 한글과 숫자 간격을 자동으로 조절하지 않음

서식 지정함: 글꼴 색: 텍스트 1

서식 지정함: 글꼴 색: 텍스트 1

서식 지정함: 글꼴 색: 텍스트 1

서식 있음: 간격 단락 뒤: 0 pt, 줄 간격: 배수 1.15 줄, 금칙 처리 안 함, 문장 부호 끝어 맞추지 않음, 한글과 영어 간격을 자동으로 조절하지 않음, 한글과 숫자 간격을 자동으로 조절하지 않음

서식 지정함: 글꼴 색: 텍스트 1

서식 지정함: 글꼴 색: 텍스트 1

서식 지정함: 글꼴 색: 텍스트 1

서식 지정함: 글꼴 색: 텍스트 1

Fan, X., Xu, Q., Scaringi, G., Dai, L., Li, W., Dong, X., ... & Havenith, H. B. (2017). Failure mechanism and kinematics of the deadly June 24th 2017 Xinmo landslide, Maoxian, Sichuan, China. Landslides, 14, 2129-2146. https://doi.org/10.1007/s10346-017-0907-7

Friedman, J. H., Hastie, T., & Tibshirani, R. (2010). Regularization paths for generalized linear models via coordinate descent. Journal of statistical software, 33, 1-22.(misquoted in the paper as Jerome 2012)

Gariano, S. L., Rianna, G., Petrucci, O., and Guzzetti, F. (2017). Assessing future changes in the occurrence of rainfall-induced landslides at a regional scale. Science of the total environment, 596, 417-426.

~~Giarola, A., Meisina, C., Tarolli, P., Zucca,~~Gelman, A. (2007). Data analysis using regression and multilevel/hierarchical models. Cambridge University Press.

~~F., Galve, J. P., and Bordoni, M. (2024). A data-driven method for the estimation of shallow landslide runout. Catena, 234, 107573.~~

Gong, Q., Wang, J., Zhou, P., and Guo, M. (2021). A regional landslide stability analysis method under the combined impact of rainfall and vegetation roots in south China. Advances in Civil Engineering, 2021, 1-12.

Gonzalez-Ollauri, A., and Mickovski, S. B. (2017). Hydrological effect of vegetation against rainfall-induced landslides. Journal of Hydrology, 549, 374-387.

Greenwood, J. R., Norris, J. E., & Wint, J. (2004). Assessing the contribution of vegetation to slope stability. Proceedings of the Institution of Civil Engineers-Geotechnical Engineering, 157(4), 199-207.

Gutierrez-Martin, A. (2020). A GIS-physically-based emergency methodology for predicting rainfall-induced shallow landslide zonation. Geomorphology, 359, 107121.

Guzzetti, F., Peruccacci, S., Rossi, M., & Stark, C. P. (2008). The rainfall intensity–duration control of shallow landslides and debris flows: an update. Landslides, 5, 3-17.

Ha, K. M. (2022). predicting typhoon tracks around Korea. Natural Hazards, 113(2), 1385-1390.

Hastie, T. (2009). The elements of statistical learning: data mining, inference, and prediction.

Highland, L. and Bobrowsky, P~~.~~. (2008), The Landslide Handbook: A Guide to Understanding Landslides, United States Geological Survey, Reston, VA, Circular 1325, https://pubs.usgs.gov/circ/1325/ (last access: 6 March 2023~~), 2008. a, b~~),

Holcombe, E. A., Beesley, M. E., Vardanega, P. J., & Sorbie, R. (2016, March). Urbanisation and landslides: hazard drivers and better practices. In Proceedings of the Institution of Civil Engineers-Civil Engineering (Vol. 169, No. 3, pp. 137-144). Thomas Telford Ltd.

Hovius, N., Stark, C. ~~P., Tutton, M. A., and Abbott, L. D. (1998). Landslide-driven drainage network evolution in~~ P., & Allen, P. A. (1997). Sediment flux from a ~~pre-steady-state~~ mountain belt~~: Finisterre Mountains, Papua New Guinea.~~ derived by landslide mapping, Geology, ~~26(12), 1071-1074~~25(3), 231-234.

Hyde, K. D., Riley, K., & Stoof, C. (2016). Uncertainties in predicting debris flow hazards following wildfire. Natural haz

서식 지정함: 글꼴 색: 텍스트 1

서식 있음: 간격 단락 뒤: 0 pt, 줄 간격: 배수 1.15 줄, 금칙 처리 안 함, 문장 부호 끝어 맞추지 않음, 한글과 영어 간격을 자동으로 조절하지 않음, 한글과 숫자 간격을 자동으로 조절하지 않음, 탭: 4.5 글자, 왼쪽

서식 지정함: 글꼴 색: 텍스트 1

서식 지정함: 글꼴 색: 텍스트 1

서식 있음: 간격 단락 뒤: 0 pt, 줄 간격: 배수 1.15 줄, 금칙 처리 안 함, 문장 부호 끝어 맞추지 않음, 한글과 영어 간격을 자동으로 조절하지 않음, 한글과 숫자 간격을 자동으로 조절하지 않음

서식 지정함: 글꼴 색: 텍스트 1

서식 있음: 간격 단락 뒤: 0 pt, 줄 간격: 배수 1.15 줄, 금칙 처리 안 함, 문장 부호 끝어 맞추지 않음, 한글과 영어 간격을 자동으로 조절하지 않음, 한글과 숫자 간격을 자동으로 조절하지 않음

서식 지정함: 글꼴 색: 텍스트 1

서식 지정함: 글꼴 색: 텍스트 1

서식 있음: 간격 단락 뒤: 0 pt, 줄 간격: 배수 1.15 줄, 금칙 처리 안 함, 문장 부호 끝어 맞추지 않음, 한글과 영어 간격을 자동으로 조절하지 않음, 한글과 숫자 간격을 자동으로 조절하지 않음, 탭: 4.5 글자, 왼쪽

서식 지정함: 글꼴 색: 텍스트 1

서식 지정함: 글꼴 색: 텍스트 1

서식 지정함: 글꼴 색: 텍스트 1

서식 지정함: 글꼴 색: 텍스트 1

서식 지정함: 글꼴 색: 텍스트 1

Hyndman, R. J., & Koehler, A. B. (2006). Another look at measures of forecast accuracy. International journal of forecasting, 22(4), 679-688.

Hyun, Y. K., Kar, S. K., Ha, K. J., & Lee, J. H. (2010). Diurnal and spatial variabilities of monsoonal CG lightning and precipitation and their association with the synoptic weather conditions over South Korea. Theoretical and applied climatology, 102, 43-60.

Intrieri, E., Carlà, T., and Gigli, G. (2019). Forecasting the time of failure of landslides at slope-scale: A literature review. Earth-science reviews, 193, 333-349.

~~Jerome Friedman, Trevor Hastie, Robert Tibshirani (2010). Regularization Paths for Generalized Linear Models via Coordinate Descent. Journal of Statistical Software, 33(1), 1-22. URL:<https://www.jstatsoft.org/v33/i01/>.~~

Islam, M. A., Islam, M. S., & Islam, T. (2017, September). Landslides in Chittagong hill tracts and possible measures. In Proceedings of the international conference on disaster risk mitigation, Dhaka, Bangladesh (Vol. 23).

Jin, H. G., Lee, H., & Baik, J. J. (2022). Characteristics and possible mechanisms of diurnal variation of summertime precipitation in South Korea. Theoretical and Applied Climatology, 148(1), 551-568.

Ju, L. Y., Zhang, L. M., and Xiao, T. (2023). Power laws for accurate determination of landslide volume based on high-resolution LiDAR data. Engineering Geology, 312, 106935.

Jung, M. J., Jeong, Y. J., Shin, W. J., & Cheong, A. C. S. (2024). Isotopic distribution of bioavailable Sr, Nd, and Pb in Chungcheongbuk-do Province, Korea. Journal of Analytical Science and Technology, 15(1), 46.

Jung, Y., Shin, J. Y., Ahn, H., and Heo, J. H. (2017). The spatial and temporal structure of extreme rainfall trends in South Korea. Water, 9(10), 809.

Kafle, L., Xu, W. J., Zeng, S. Y., & Nagel, T. (2022). A numerical investigation of slope stability influenced by the combined effects of reservoir water level fluctuations and precipitation: A case study of the Bianjiazhai landslide in China. Engineering Geology, 297, 106508.

Kang, M. W., Yibeltal, M., Kim, Y. H., Oh, S. J., Lee, J. C., Kwon, E. E., & Lee, S. S. (2022). Enhancement of soil physical properties and soil water retention with biochar-based soil amendments. Science of the total environment, 836, 155746.

Keefer, R. F. (2000). Handbook of soils for landscape architects. Oxford University Press.

Khan, M. A., Basharat, M., Riaz, M. T., Sarfraz, Y., Farooq, M., Khan, A. Y., ... and Shahzad, A. (2021). An integrated geotechnical and geophysical investigation of a catastrophic landslide in the Northeast Himalayas of Pakistan. Geological Journal, 56(9), 4760-4778.

Khan, Y. A., Lateh, H., Baten, M. A., and Kamil, A. A. (2012). Critical antecedent rainfall conditions for shallow landslides in Chittagong City of Bangladesh. Environmental Earth Sciences, 67, 97-106.

Kim, D. E., Seong, Y. B., Weber, J., & Yu, B. Y. (2020). Unsteady migration of Taebaek Mountain drainage divide, Cenozoic extensional basin margin, Korean Peninsula. Geomorphology, 352, 107012.

서식 있음: 간격 단락 뒤: 0 pt, 줄 간격: 배수 1.15 줄, 금칙 처리 안 함, 문장 부호 끌어 맞추지 않음, 한글과 영어 간격을 자동으로 조절하지 않음, 한글과 숫자 간격을 자동으로 조절하지 않음, 탭: 4.5 글자, 왼쪽

서식 지정함: 글꼴 색: 텍스트 1

서식 지정함: 글꼴 색: 텍스트 1

서식 있음: 간격 단락 뒤: 0 pt, 줄 간격: 배수 1.15 줄, 금칙 처리 안 함, 문장 부호 끌어 맞추지 않음, 한글과 영어 간격을 자동으로 조절하지 않음, 한글과 숫자 간격을 자동으로 조절하지 않음

서식 지정함: 글꼴 색: 텍스트 1

서식 있음: 간격 단락 뒤: 0 pt, 줄 간격: 배수 1.15 줄, 금칙 처리 안 함, 문장 부호 끌어 맞추지 않음, 한글과 영어 간격을 자동으로 조절하지 않음, 한글과 숫자 간격을 자동으로 조절하지 않음

서식 지정함: 글꼴 색: 텍스트 1

서식 있음: 간격 단락 뒤: 0 pt, 줄 간격: 배수 1.15 줄, 금칙 처리 안 함, 문장 부호 끌어 맞추지 않음, 한글과 영어 간격을 자동으로 조절하지 않음, 한글과 숫자 간격을 자동으로 조절하지 않음

서식 지정함: 글꼴 색: 텍스트 1

Kim, H. G., & Park, C. Y. (2021). Landslide susceptibility analysis of photovoltaic power stations in Gangwon-do, Republic of Korea. Geomatics, Natural Hazards and Risk, 12(1), 2328-2351.

Kim, J., Lee, K., Jeong, S., & Kim, G. (2014). GIS-based prediction method of landslide susceptibility using a rainfall infiltration-groundwater flow model. Engineering geology, 182, 63-78.

Kim, M. S., Onda, Y., Kim, J. K., & Kim, S. W. (2015). Effect of topography and soil parameterisation representing soil thicknesses on shallow landslide modelling. Quaternary International, 384, 91-106.

Kim, S. W., Chun, K. W., Kim, M., Catani, F., Choi, B., and Seo, J. I. (2021). Effect of antecedent rainfall conditions and their variations on shallow landslide-triggering rainfall thresholds in South Korea. Landslides, 18, 569-582.

Kitutu, M. G., Muwanga, A., Poesen, J., and Deckers, J. A. (2009). Influence of soil properties on landslide occurrences in Bududa district, Eastern Uganda. African journal of agricultural research, 4(7), 611-620.

Klimeš, J., Stemberk, J., Blahut, J., Krejčí, V., Krejčí, O., Hartvich, F., & Kycl, P. (2017). Challenges for landslide hazard and risk management in 'low-risk'regions, Czech Republic—landslide occurrences and related costs (IPL project no. 197). Landslides, 14, 771-780

Korup, O., Clague, J. J., Hermanns, R. L., Hewitt, K., Strom, A. L., and Weidinger, J. T. (2007). Giant landslides, topography, and erosion. Earth and Planetary Science Letters, 261(3-4), 578-589.

Kramer, O., and Kramer, O. (2013). K-nearest neighbors. Dimensionality reduction with unsupervised nearest neighbors, 13-23.

Krizhevsky, A., Sutskever, I., & Hinton, G. E. (2012). Imagenet classification with deep convolutional neural networks. Advances in neural information processing systems, 25.

Kuhn M (2022). –caret: Classification and Regression Training_. R package version 6.0-92, <https://CRAN.R-project.org/package=caret>

Kunz, M., & Kottmeier, C. (2006). Orographic enhancement of precipitation over low mountain ranges. Part II: Simulations of heavy precipitation events over southwest Germany. Journal of applied meteorology and climatology, 45(8), 1041-1055.

Lacerda, W. A., Palmeira, E. M., Netto, A. L. C., & Ehrlich, M. (Eds.). (2014). Extreme rainfall induced landslides: an international perspective. Oficina de Textos.

Lann, T., Bao, H., Lan, H., Zheng, H., & Yan, C. (2024). Hydro-mechanical effects of vegetation on slope stability: A review. Science of the Total Environment, 171691.

LeCun, Y., Bengio, Y., and Hinton, G. (2015). Deep learning. nature, 521(7553), 436-444.

Lee, D. B., Kim, Y. N., Sonn, Y. K., & Kim, K. H. (2023). Comparison of Soil Taxonomy (2022) and WRB (2022) Systems for classifying Paddy Soils with different drainage grades in South Korea. Land, 12(6), 1204.

서식 지정함: 글꼴 색: 텍스트 1

서식 있음: 간격 단락 뒤: 0 pt, 줄 간격: 배수 1.15 줄, 금칙 처리 안 함, 문장 부호 끝어 맞추지 않음, 한글과 영어 간격을 자동으로 조절하지 않음, 한글과 숫자 간격을 자동으로 조절하지 않음

서식 지정함: 글꼴 색: 텍스트 1

서식 있음: 간격 단락 뒤: 0 pt, 줄 간격: 배수 1.15 줄, 금칙 처리 안 함, 문장 부호 끝어 맞추지 않음, 한글과 영어 간격을 자동으로 조절하지 않음, 한글과 숫자 간격을 자동으로 조절하지 않음

서식 지정함: 글꼴 색: 텍스트 1

서식 지정함: 글꼴 색: 텍스트 1

서식 있음: 간격 단락 뒤: 0 pt, 줄 간격: 배수 1.15 줄, 금칙 처리 안 함, 문장 부호 끝어 맞추지 않음, 한글과 영어 간격을 자동으로 조절하지 않음, 한글과 숫자 간격을 자동으로 조절하지 않음

서식 지정함: 글꼴 색: 텍스트 1

서식 지정함: 글꼴 색: 텍스트 1

서식 지정함: 글꼴 색: 텍스트 1

서식 지정함: 글꼴 색: 텍스트 1

서식 있음: 간격 단락 뒤: 0 pt, 줄 간격: 배수 1.15 줄, 금칙 처리 안 함, 문장 부호 끝어 맞추지 않음, 한글과 영어 간격을 자동으로 조절하지 않음, 한글과 숫자 간격을 자동으로 조절하지 않음

Lee, D. H., Cheon, E., Lim, H. H., Choi, S. K., Kim, Y. T., ~~and~~& Lee, S. R. (2021). An artificial neural network model to predict debris-flow volumes caused by extreme rainfall in the central region of South Korea. Engineering Geology, 281, 105979.

Lee, D. H., Kim, Y. T., and Lee, S. R. (2020). Shallow landslide susceptibility models based on artificial neural networks considering the factor selection method and various non-linear activation functions. Remote Sensing, 12(7), 1194.

Lee, J. U., Cho, Y. C., Kim, M., Jang, S. J., Lee, J., & Kim, S. (2022). The effects of different geological conditions on landslide-triggering rainfall conditions in South Korea. Water, 14(13), 2051.

Lee, M. J. (2016). Rainfall and landslide correlation analysis and prediction of future rainfall base on climate change. In Geohazards Caused by Human Activity. IntechOpen.

Lee, S. G. (2009). The Effects of Landslide in South Korea and Some Issues for Successful Management and Mitigation. 한국토양비료학회 학술발표회 초록집, 181-191.

Lee, S. ~~G., and Winter, M. G. (2019). The effects of debris flow in the Republic of Korea and some issues for successful risk reduction. Engineering geology, 251, 172-189.~~

~~Lee, S.~~ W., Kim, G., Yune, C. Y., and Ryu, H. J. (2013). Development of landslide-risk assessment model for mountainous regions in eastern Korea. Disaster ~~advances~~Advances, 6(6), 70-79.

Li, B. V., Jenkins, C. N., & Xu, W. (2022a). Strategic protection of landslide vulnerable mountains for biodiversity conservation under land-cover and climate change impacts. Proceedings of the National Academy of Sciences, 119(2), e2113416118.

Li, C. J., Guo, C. X., Yang, X. G., Li, H. B., & Zhou, J. W. (2022b). A GIS-based probabilistic analysis model for rainfall-induced shallow landslides in mountainous areas. Environmental Earth Sciences, 81(17), 432.

Liaw, A., and Wiener, M., (2002). Classification and regression by randomForest. R News 2(3), 18--22.

Liu, Y., Deng, Z., & Wang, X. (2021). The effects of rainfall, soil type and slope on the processes and mechanisms of rainfall-induced shallow landslides. Applied Sciences, 11(24), 11652.

Luino, F., De Graff, J., Biddoccu, M., Faccini, F., Freppaz, M., Roccati, A., ... & Turconi, L. (2022). The Role of soil type in triggering shallow landslides in the alps (Lombardy, Northern Italy). Land, 11(8), 1125.

Lusiana, N., Shinohara, Y., & Imaizumi, F. (2024). Quantifying effects of changes in forest age distribution on the landslide frequency in Japan. Natural Hazards, 1-20.

Martinović, K., Gavin, K., Reale, C., and Mangan, C. (2018). Rainfall thresholds as a landslide indicator for engineered slopes on the Irish Rail network. Geomorphology, 306, 40-50.

Mateos, R. M., López-Vinielles, J., Poyiadji, E., Tsagkas, D., Sheehy, M., Hadjicharalambous, K., ... & Herrera, G. (2020). Integration of landslide hazard into urban planning across Europe. Landscape and urban planning, 196, 103740.

서식 지정함: 글꼴 색: 텍스트 1

서식 지정함: 글꼴 색: 텍스트 1

서식 있음: 간격 단락 뒤: 0 pt, 줄 간격: 배수 1.15 줄, 금칙 처리 안 함, 문장 부호 끝어 맞추지 않음, 한글과 영어 간격을 자동으로 조절하지 않음, 한글과 숫자 간격을 자동으로 조절하지 않음

서식 지정함: 글꼴 색: 텍스트 1

서식 있음: 간격 단락 뒤: 0 pt, 줄 간격: 배수 1.15 줄, 금칙 처리 안 함, 문장 부호 끝어 맞추지 않음, 한글과 영어 간격을 자동으로 조절하지 않음, 한글과 숫자 간격을 자동으로 조절하지 않음

서식 지정함: 글꼴 색: 텍스트 1

서식 지정함: 글꼴 색: 텍스트 1

서식 있음: 간격 단락 뒤: 0 pt, 줄 간격: 배수 1.15 줄, 금칙 처리 안 함, 문장 부호 끝어 맞추지 않음, 한글과 영어 간격을 자동으로 조절하지 않음, 한글과 숫자 간격을 자동으로 조절하지 않음, 탭: 4.5 글자, 왼쪽

서식 지정함: 글꼴 색: 텍스트 1

서식 지정함: 글꼴 색: 텍스트 1

서식 있음: 간격 단락 뒤: 0 pt, 줄 간격: 배수 1.15 줄, 금칙 처리 안 함, 문장 부호 끝어 맞추지 않음, 한글과 영어 간격을 자동으로 조절하지 않음, 한글과 숫자 간격을 자동으로 조절하지 않음

서식 지정함: 글꼴 색: 텍스트 1

서식 있음: 간격 단락 뒤: 0 pt, 줄 간격: 배수 1.15 줄, 금칙 처리 안 함, 문장 부호 끝어 맞추지 않음, 한글과 영어 간격을 자동으로 조절하지 않음, 한글과 숫자 간격을 자동으로 조절하지 않음

McKenna, J. P., Santi, P. M., Amblard, X., and Negri, J. (2012). Effects of soil-engineering properties on the failure mode of shallow landslides. Landslides, 9, 215-228.

McKight, P. E., and Najab, J. (2010). Kruskal-wallis test. The corsini encyclopedia of psychology, 1-1.

~~Melo, R., Zêzere, J. L., Rocha, J., and Oliveira, S. C. (2019). Combining data-driven models to assess susceptibility of shallow slides failure and runout. Landslides, 16, 2259-2276.~~

Meyer D, Dimitriadou E, Hornik K, Weingessel A, Leisch F (2021). _e1071: Misc Functions of the Department of Statistics, Probability Theory Group (Formerly: E1071), TU Wien_. R package version 1.7-9, <https://CRAN.R-project.org/package=e1071>.

Miao, F., Wu, Y., Xie, Y., and Li, Y. (2018). Prediction of landslide displacement with step-like behavior based on multialgorithm optimization and a support vector regression model. Landslides, 15, 475-488.

Nguyen, Q. H., Ly, H. B., Ho, L. S., Al-Ansari, N., Le, H. V., Tran, V. Q., ... & Pham, B. T. (2021). Influence of data splitting on performance of machine learning models in prediction of shear strength of soil. Mathematical Problems in Engineering, 2021(1), 4832864.

O'brien, R. M. (2007). A caution regarding rules of thumb for variance inflation factors. Quality and quantity, 41, 673-690.

Omwega, A. K. (1989). Crop cover, rainfall energy and soil erosion in Githunguri (Kiambu District), Kenya. The University of Manchester (United Kingdom).

Panday, S., & Dong, J. J. (2021). Topographical features of rainfall-triggered landslides in Mon State, Myanmar, August 2019: Spatial distribution heterogeneity and uncommon large relative heights. Landslides, 18(12), 3875-3889.

Park, C. Y. (2015). The classification of extreme climate events in the Republic of Korea. Journal of the Korean association of regional geographers, 21(2), 394-410.

Park, S. J., & Lee, D. K. (2021). Predicting susceptibility to landslides under climate change impacts in metropolitan areas of South Korea using machine learning. Geomatics, Natural Hazards and Risk, 12(1), 2462-2476.

Park, S.J. (2022). Assessment of disaster risks induced by climate change, using machine learning techniques (Doctoral dissertation, 서울대학교 대학원).

Paudel, P. P., Omura, H., Kubota, T., and Morita, K. (2003). Landslide damage and disaster management system in Nepal. Disaster Prevention and Management: An International Journal, 12(5), 413-419.

~~Peruzzetto, M., Mangeney, A., Grandjean, G., Levy, C., Thiery, Y., Rohmer, J., and Lucas, A. (2020). Operational estimation of landslide runout: comparison of empirical and numerical methods. Geosciences, 10(11), 424.~~

Pham, B. T., Tien Bui, D., and Prakash, I. (2018). Bagging based support vector machines for spatial prediction of landslides. Environmental Earth Sciences, 77, 1-17.

서식 지정함: 글꼴 색: 텍스트 1

서식 있음: 간격 단락 뒤: 0 pt, 줄 간격: 배수 1.15 줄, 금칙 처리 안 함, 문장 부호 끌어 맞추지 않음, 한글과 영어 간격을 자동으로 조절하지 않음, 한글과 숫자 간격을 자동으로 조절하지 않음, 탭: 4.5 글자, 왼쪽

서식 지정함: 글꼴 색: 텍스트 1

서식 지정함: 글꼴 색: 텍스트 1, 프랑스어(프랑스)

서식 지정함: 글꼴 색: 텍스트 1

서식 있음: 간격 단락 뒤: 0 pt, 줄 간격: 배수 1.15 줄, 금칙 처리 안 함, 문장 부호 끌어 맞추지 않음, 한글과 영어 간격을 자동으로 조절하지 않음, 한글과 숫자 간격을 자동으로 조절하지 않음

서식 지정함: 글꼴 색: 텍스트 1, 영어(미국)

서식 지정함: 글꼴 색: 텍스트 1

서식 지정함: 글꼴 색: 텍스트 1

서식 있음: 간격 단락 뒤: 0 pt, 줄 간격: 배수 1.15 줄, 금칙 처리 안 함, 문장 부호 끌어 맞추지 않음, 한글과 영어 간격을 자동으로 조절하지 않음, 한글과 숫자 간격을 자동으로 조절하지 않음

서식 지정함: 글꼴 색: 텍스트 1

서식 있음: 간격 단락 뒤: 0 pt, 줄 간격: 배수 1.15 줄, 금칙 처리 안 함, 문장 부호 끌어 맞추지 않음, 한글과 영어 간격을 자동으로 조절하지 않음, 한글과 숫자 간격을 자동으로 조절하지 않음

서식 지정함: 글꼴 색: 텍스트 1

서식 있음: 간격 단락 뒤: 0 pt, 줄 간격: 배수 1.15 줄, 금칙 처리 안 함, 문장 부호 끌어 맞추지 않음, 한글과 영어 간격을 자동으로 조절하지 않음, 한글과 숫자 간격을 자동으로 조절하지 않음

Phillips, C., Hales, T., Smith, H., and Basher, L. (2021). Shallow landslides and vegetation at the catchment scale: A perspective. Ecological Engineering, 173, 106436.

Pisner, D. A., and Schnyer, D. M. (2020). Support vector machine. In Machine learning (pp. 101-121). Academic Press.

Pradhan, S., Toll, D. G., Rosser, N. J., & Brain, M. J. (2022). An investigation of the combined effect of rainfall and road cut on landsliding. Engineering Geology, 307, 106787. https://doi.org/10.1016/j.enggeo.2022.106787

Qiu, H., Regmi, A. D., Cui, P., Cao, M., Lee, J., and Zhu, X. (2016). Size distribution of loess slides in relation to local slope height within different slope morphologies. Catena, 145, 155-163.

R Core Team (2022). R: A language and environment for statistical computing. R Foundation for Statistical Computing, Vienna, Austria. URL: <https://www.R-project.org/>.

Rahman, M. S., Ahmed, B., & Di, L. (2017). Landslide initiation and runout susceptibility modeling in the context of hill cutting and rapid urbanization: a combined approach of weights of evidence and spatial multi-criteria. Journal of Mountain Science, 14(10), 1919-1937.

Ran, Q., Wang, J., Chen, X., Liu, L., Li, J., & Ye, S. (2022). The relative importance of antecedent soil moisture and precipitation in flood generation in the middle and lower Yangtze River basin. Hydrology and Earth System Sciences, 26(19), 4919-4931.

Rathore, S. S., and Kumar, S. (2016). A decision tree regression-based approach for the number of software faults prediction. ACM SIGSOFT Software Engineering Notes, 41(1), 1-6.

Razakova, M., Kuzmin, A., Fedorov, I., Yergaliev, R., and Ainakulov, Z. (2020). Methods of calculating landslide volume using remote sensing data. In E3S Web of Conferences (Vol. 149, p. 02009). EDP Sciences.

Rosi, A., Peternel, T., Jemec-Auflič, M., Komac, M., Segoni, S., and Casagli, N. (2016). Rainfall thresholds for rainfall-induced landslides in Slovenia. Landslides, 13, 1571-1577.

Rotaru, A., Oajdea, D., and Răileanu, P. (2007). Analysis of the landslide movements. International journal of geology, 1(3), 70-79.

Saito, H., Korup, O., Uchida, T., Hayashi, S., & Oguchi, T. (2014). Rainfall conditions, typhoon frequency, and contemporary landslide erosion in Japan. Geology, 42(11), 999-1002.

Saleh, A. M. E., Arashi, M., and Kibria, B. G. (2019). Theory of ridge regression estimation with applications. John Wiley and Sons.

Sato, T., Katsuki, Y., & Shuin, Y. (2023). Evaluation of influences of forest cover change on landslides by comparing rainfall-induced landslides in Japanese artificial forests with different ages. Scientific reports, 13(1), 14258.

Scheidl, C., Heiser, M., Kamper, S., Thaler, T., Klebinder, K., Nagl, F., ... and Seidl, R. (2020). The influence of climate change and canopy disturbances on landslide susceptibility in headwater catchments. Science of the total environment, 742, 140588.

Seger, C. (2018). An investigation of categorical variable encoding techniques in machine learning: binary versus one-hot and feature hashing.

서식 지정함: 글꼴 색: 텍스트 1

서식 있음: 간격 단락 뒤: 0 pt, 줄 간격: 배수 1.15 줄, 금칙 처리 안 함, 문장 부호 끝어 맞추지 않음, 한글과 영어 간격을 자동으로 조절하지 않음, 한글과 숫자 간격을 자동으로 조절하지 않음

서식 지정함: 글꼴 색: 텍스트 1

서식 있음: 간격 단락 뒤: 0 pt, 줄 간격: 배수 1.15 줄, 금칙 처리 안 함, 문장 부호 끝어 맞추지 않음, 한글과 영어 간격을 자동으로 조절하지 않음, 한글과 숫자 간격을 자동으로 조절하지 않음

서식 지정함: 글꼴 색: 텍스트 1

서식 있음: 간격 단락 뒤: 0 pt, 줄 간격: 배수 1.15 줄, 금칙 처리 안 함, 문장 부호 끝어 맞추지 않음, 한글과 영어 간격을 자동으로 조절하지 않음, 한글과 숫자 간격을 자동으로 조절하지 않음

서식 지정함: 글꼴 색: 텍스트 1

서식 있음: 간격 단락 뒤: 0 pt, 줄 간격: 배수 1.15 줄, 금칙 처리 안 함, 문장 부호 끝어 맞추지 않음, 한글과 영어 간격을 자동으로 조절하지 않음, 한글과 숫자 간격을 자동으로 조절하지 않음

Singh, D., and Singh, B. (2022). Feature wise normalization: An effective way of normalizing data. Pattern Recognition, 122, 108307.
Smith, H. G., Neverman, A. J., Betts, H., & Spiekermann, R. (2023). The influence of spatial patterns in rainfall on shallow landslides. Geomorphology, 437, 108795.
Spiker, E. C., & Gori, P. (2003). National landslide hazards mitigation strategy, a framework for loss reduction (No. 1244). US Geological Survey.
Stoof, C. R., Vervoort, R. W., Iwema, J., Van Den Elsen, E., Ferreira, A. J. D., & Ritsema, C. J. (2012). Hydrological response of a small catchment burned by experimental fire. Hydrology and Earth System Sciences, 16(2), 267-285.
Sun, H. Y., Wong, L. N. Y., Shang, Y. Q., Shen, Y. J., and Lü, Q. (2010). Evaluation of drainage tunnel effectiveness in landslide control. Landslides, 7, 445-454.
Székely, G. J., Rizzo, M. L., and Bakirov, N. K. (2007). Measuring and testing dependence by correlation of distances.
Tacconi Stefanelli, C., Casagli, N., & Catani, F. (2020). Landslide damming hazard susceptibility maps: a new GIS-based procedure for risk management. Landslides, 17, 1635-1648.
Tsai, T. L., & Chen, H. F. (2010). Effects of degree of saturation on shallow landslides triggered by rainfall. Environmental Earth Sciences, 59, 1285-1295.
Turner, T. R., Duke, S. D., Fransen, B. R., Reiter, M. L., Kroll, A. J., Ward, J. W., ... ~~and~~& Bilby, R. E. (2010). Landslide densities associated with rainfall, stand age, and topography on forested landscapes, southwestern Washington, USA. Forest Ecology and Management, 259(12), 2233-2247.
Um, M. J., Yun, H., Cho, W., & Heo, J. H. (2010). Analysis of orographic precipitation on Jeju-Island using regional frequency analysis and regression. Water resources management, 24, 1461-1487.
Van Tien, P., Luong, L. H., Duc, D. M., Trinh, P. T., Quynh, D. T., Lan, N. C., ... & Loi, D. H. (2021). Rainfall-induced catastrophic landslide in Quang Tri Province: the deadliest single landslide event in Vietnam in 2020.
Wang, D., Hollaus, M., Schmaltz, E., Wieser, M., Reifeltshammer, D., & Pfeifer, N. (2016). Tree stem shapes derived from TLS data as an indicator for shallow landslides. Procedia Earth and Planetary Science, 16, 185-194.
Wei, Z. L., Shang, Y. Q., Sun, H. Y., Xu, H. D., and Wang, D. F. (2019). The effectiveness of a drainage tunnel in increasing the rainfall threshold of a deep-seated landslide. Landslides, 16, 1731-1744.
Wieczorek, G. (1987). In central Santa Cruz Mountains, California. Debris flows/avalanches: process, recognition, and mitigation, 7, 93.
Willmott, C. J., & Matsuura, K. (2005). Advantages of the mean absolute error (MAE) over the root mean square error (RMSE) in assessing average model performance. Climate research, 30(1), 79-82.
Winter, M. G., & Bromhead, E. N. (2012). Landslide risk: some issues that determine societal acceptance. Natural Hazards, 62, 169-187.

서식 지정함: 글꼴 색: 텍스트 1

서식 있음: 간격 단락 뒤: 0 pt, 줄 간격: 배수 1.15 줄, 금칙 처리 안 함, 문장 부호 끝어 맞추지 않음, 한글과 영어 간격을 자동으로 조절하지 않음, 한글과 숫자 간격을 자동으로 조절하지 않음

서식 지정함: 글꼴 색: 텍스트 1

서식 지정함: 글꼴 색: 텍스트 1

서식 있음: 간격 단락 뒤: 0 pt, 줄 간격: 배수 1.15 줄, 금칙 처리 안 함, 문장 부호 끝어 맞추지 않음, 한글과 영어 간격을 자동으로 조절하지 않음, 한글과 숫자 간격을 자동으로 조절하지 않음, 탭: 4.5 글자, 왼쪽

서식 지정함: 글꼴 색: 텍스트 1, 프랑스어(프랑스)

서식 있음: 간격 단락 뒤: 0 pt, 줄 간격: 배수 1.15 줄, 금칙 처리 안 함, 문장 부호 끝어 맞추지 않음, 한글과 영어 간격을 자동으로 조절하지 않음, 한글과 숫자 간격을 자동으로 조절하지 않음

서식 지정함: 글꼴 색: 텍스트 1

서식 지정함: 글꼴 색: 텍스트 1

서식 있음: 간격 단락 뒤: 0 pt, 줄 간격: 배수 1.15 줄, 금칙 처리 안 함, 문장 부호 끝어 맞추지 않음, 한글과 영어 간격을 자동으로 조절하지 않음, 한글과 숫자 간격을 자동으로 조절하지 않음

서식 지정함: 글꼴 색: 텍스트 1

Yan, L., Xu, W., Wang, H., Wang, R., Meng, Q., Yu, J., and Xie, W. C. (2019). Drainage controls on the Donglingxing landslide (China) induced by rainfall and fluctuation in reservoir water levels. Landslides, 16, 1583-1593.

Yang, H., & Adler, R. F. (2008). Predicting global landslide spatiotemporal distribution: integrating landslide susceptibility zoning techniques and real-time satellite rainfall estimates. International Journal of Sediment Research, 23(3), 249-257.

Yoon, S. S., & Bae, D. H. (2013). Optimal rainfall estimation by considering elevation in the Han River Basin, South Korea. Journal of Applied Meteorology and Climatology, 52(4), 802-818.

Yun, H. S., Um, M. J., Cho, W. C., & Heo, J. H. (2009). Orographic precipitation analysis with regional frequency analysis and multiple linear regression. Journal of Korea Water Resources Association, 42(6), 465-480.

Yune, C. Y., Jun, K. J., Kim, K. S., Kim, G. H., and Lee, S. W. (2010). Analysis of slope hazard-triggering rainfall characteristics in Gangwon Province by database construction. Journal of the Korean Geotechnical Society, 26(10), 27-38.

Zachar, D. (2011). Soil erosion. Elsevier.

Zaruba, Q., and Mencl, V. (2014). Landslides and their control. Elsevier.

Zhang, K., Wang, S., Bao, H., & Zhao, X. (2019). Characteristics and influencing factors of rainfall-induced landslide and debris flow hazards in Shaanxi Province, China. Natural Hazards and Earth System Sciences, 19(1), 93-105.

서식 지정함: 글꼴 색: 텍스트 1

서식 있음: 간격 단락 뒤: 0 pt, 줄 간격: 배수 1.15 줄, 금칙 처리 안 함, 문장 부호 끌어 맞추지 않음, 한글과 영어 간격을 자동으로 조절하지 않음, 한글과 숫자 간격을 자동으로 조절하지 않음

서식 지정함: 글꼴 색: 텍스트 1

서식 있음: 간격 단락 뒤: 0 pt, 줄 간격: 배수 1.15 줄, 금칙 처리 안 함, 문장 부호 끌어 맞추지 않음, 한글과 영어 간격을 자동으로 조절하지 않음, 한글과 숫자 간격을 자동으로 조절하지 않음

서식 지정함: 글꼴 색: 텍스트 1

서식 있음: 간격 단락 뒤: 0 pt, 줄 간격: 배수 1.15 줄, 금칙 처리 안 함, 문장 부호 끌어 맞추지 않음, 한글과 영어 간격을 자동으로 조절하지 않음, 한글과 숫자 간격을 자동으로 조절하지 않음, 탭: 4.5 글자, 왼쪽

서식 지정함: 글꼴: 굵게, 글꼴 색: 텍스트 1

서식 있음: 들여쓰기: 왼쪽: 0 cm, 첫 줄: 0 cm, 간격 단락 뒤: 0 pt, 단락의 첫 줄이나 마지막 줄 분리 허용, 단어 잘림 허용, 한글과 영어 간격을 자동으로 조절하지 않음, 한글과 숫자 간격을 자동으로 조절하지 않음